Freeze-drying of drug nanosuspension– study of formulation and processing factors for the optimization and characterization of redispersible cilostazol nanocrystals

Emilia Jakubowska [a,*], Michał Bielejewski [b], Bartłomiej Milanowski [a], Janina Lulek [a,**]

[a] Chair and Department of Pharmaceutical Technology, Faculty of Pharmacy, Poznan University of Medical Sciences, 6 Grunwaldzka Street, 60-780, Poznan, Poland
[b] Institute of Molecular Physics, Polish Academy of Sciences, 17 M. Smoluchowskiego Street, 60-179, Poznan, Poland

A B S T R A C T

The aim of this work was to systematically study the effect of freeze-drying of bottom-up processed cilostazol nanosuspension on the particle size after redispersion. Several different cryoprotectants and concentrations were compared and the influence of processing variables such as freezing temperature, cooling rate and primary drying temperature was systematically and thoroughly evaluated in combinations across the matrix former range and their concentrations to establish their impact on nanocrystal size. As a result, optimal settings for the lyophilization of cilostazol nanosuspensions were identified in terms of good redispersibility and acceptable cake appearance. Selected optimal formulations containing 10% trehalose, 5% maltodextrin or 10% PEG 1500 were further characterized with respect to sample morphology, solid state and residual content of moisture (0.4–1.0%) and DMSO (0–13%). The freeze-dried nanocrystals successfully preserved not only their original size (d50 = 0.366–0.453 μm and d90 = 1.68–2.82 μm, depending on the matrix former) and polymorphic form A of cilostazol, but also the improved dissolution rate (over 90% of the drug dissolved in 5 min vs. less than 30% dissolved from raw, untreated cilostazol in 60 min). Moreover, the study addressed the specific problems related to the presence of organic solvent (DMSO) when freeze-drying nanosuspensions developed with bottom-up precipitation methods.

1. Introduction

Drug nanocrystals are one of technologies used for the improvement of dissolution rate and bioavailability of poorly soluble active pharmaceutical ingredients (APIs), which is a major challenge in contemporary drug and formulation development. Particle size reduction to nanoscale is commonly performed in liquid environment, either in top-down processes involving the mechanical comminution of a solid (wet media milling, high pressure homogenization), or in bottom-up precipitation processes [1,2]. Consequently, newly produced nanocrystals exist in the form of nanosuspension, which needs to be subjected to downstream processing into solid particles for the most popular applications, i.e. solid oral dosage forms or reconstituted powders for parenteral administration. Methods of nanosuspension solidification, such as freeze-drying, spray drying, fluid bed drying, bead layering or various granulation methods have been reviewed in several papers [3–5].

Regardless of the employed downstream process, the major concern in its optimization is the retention of the original nanosuspension particle size distribution generally below 1 μm (or, according to some classifications, the values of d50 < 1 μm and d90 < 2.5 μm) [5]. In other words, care must be taken to avoid nanoparticle aggregation or fusion induced by thermal stress and the removal of liquid phase. Another consideration is potential conversion of an API's crystalline form into another polymorph, or crystallization of its amorphous form and vice versa during drying, which could impact the drug's stability or solubility. Therefore, both the formulation (choice of matrix or carrier excipient, their concentration) and the operating parameters of the drying process must be studied and optimized with the aim to reproduce the original nanocrystals' size and solid state properties in order to preserve the improved dissolution rate over non-nanosized drug. Depending on the intended application, consideration should also be given to other

---

* Corresponding author.
** Corresponding author.

E-mail addresses: ejakubowska@ump.edu.pl (E. Jakubowska), jlulek@ump.edu.pl (J. Lulek).

aspects, for instance flowability of the powder, reconstitution time or residual moisture.

Of the aforementioned solidification methods for nanosuspensions, freeze-drying appears to be the most commonly reported in the publicly available literature [3,6–8], despite its practical disadvantages such as long processing times or high energy consumption [9]; moreover, it is also used as drying method for other types of nanoparticulate systems apart from drug nanocrystals [10,11]. Since lyophilization process consists of freezing the liquid material and subsequent sublimation of the solvent under reduced pressure (sometimes followed by secondary drying to desorb the unfrozen water), it is suitable for thermally sensitive materials. On the other hand, the same principle introduces certain complexity to the challenge of maintaining nanocrystals' size stability, as particles may aggregate during two parts of the process. First, the cryogenic stress related to the confinement of nanoparticles to interstitial spaces between frozen crystals may force them to aggregate during the freezing stage because of the reduced distance. Second, agglomeration or fusion might take place during the removal of frozen solvent. In consequence, several processing factors in lyophilization may affect the size of dried and redispersed nanocrystals: freezing stress as determined by the cooling rate and temperature, as well as freezing front propagation behavior dependent on the equipment used (lyophilizer shelf, deep freezer, quench cooling in liquid nitrogen etc.), and primary drying intensity (as governed by vacuum, shelf temperature and time). More importantly, formulation factors of lyophilized nanosuspension appear to be even more impactful on their redispersibility than processing variables [11]. These factors may even involve the top-down or bottom-up step of nanoparticle production preceding freeze-drying itself, as demonstrated by the dependence of redispersion on the choice and concentration of stabilizer used in liquid nanosuspension [12–16], as well as on the drug load [12,17]. The presence of cryoprotectant/lyoprotectant or matrix former is generally essential for preventing nanocrystal aggregation, with its type and concentration significantly affecting the results, although there have been examples of successful freeze-dried nanocrystals where no additional excipients were necessary [18,19]. These formulation and processing factors exhibit a complex interplay (Fig. 1), which is convoluted even further by the fact that the abovementioned variables exert varied influence on different drugs, where a compound's hydrophobicity is correlated to its tendency to aggregate during lyophilization [20,21]. This undoubtedly is one of the reasons why the study of freeze-drying effects on nanocrystals behavior and process optimization so far has been mostly empirical [11].

In this context, new investigations into nanocrystal freeze-drying processes not yet described seems warranted as a means to expand the knowledge base. This is the case for cilostazol (further referred to as CIL), an antiplatelet drug used in the treatment of intermittent claudication. Although several nanosuspensions of this poorly soluble

Biopharmaceutics Classification System (BCS) class II compound have been described [22–26], the reports on their solidification are rather scarce and involve such methods as centrifugation or filtration [27], spray drying [28–30], vacuum drying [31] or pellet loading [32]. In one study, freeze-drying of a wet milled cilostazol nanosuspension is only briefly mentioned as a way to obtain solid samples for XRPD and DSC studies, but no details on the process or its effect on particle size are given [33].

Therefore, the aim of this work is to systematically study the influence of lyophilization processing parameters on the redispersed particles' size for cilostazol nanosuspension previously developed with an optimized liquid antisolvent precipitation-sonication method [34]. The effect of cryoprotectant type and concentration, freezing temperatures, cooling rate and primary drying temperature on redispersibility is thoroughly explored, and selected formulations are further characterized with respect to the lyophilizate morphology, solid state properties, residual solvent and water levels, and finally, the *in vitro* dissolution behavior of cilostazol. Although there exist numerous studies on freeze-drying of drug nanosuspensions investigating the aforementioned parameters and their relation to nanocrystals' size, they usually focus on a select narrow aspect (e.g. separate consideration of freezing stage or cryoprotectant choice) [12,35–40], employ OFAT (one factor at a time approach) [14,16,21,41,42] or rely on custom/non-standard lyophilization equipment [19,43,44]. The current study aims for a slightly more holistic approach, where potential interactions between variables could be observed and formulation behavior within different sets of freeze-drying conditions could be explored, allowing to determine how different processing temperatures and rates affect cilostazol nanocrystals size when lyophilized with various matrices. Consideration is also given to the question of non-aqueous solvent removal in the process itself, specific to nanosuspensions produced by bottom-up methods, which, to the authors' knowledge, has rarely been addressed directly in the publicly available literature.

2. Materials and methods

2.1. Materials

Cilostazol supplied by Glenmark (Mumbai, India) was kindly donated by Przedsiębiorstwo Farmaceutyczne Lek-Am Sp. z o.o. All other materials of p.a. grade were purchased from commercial sources, namely Chempur (Piekary Śląskie, Poland): dimethyl sulfoxide (DMSO), sucrose, glucose monohydrate, lactose monohydrate, D-fructose, glycine, gum arabic; Sigma Aldrich (Merck Life Science, Poznan, Poland): poly(vinyl alcohol) (PVA) MW 9–10 kDa 80% hydrolyzed, methanol for HPLC 99.9%; Pol-Aura (Dywity, Poland): trehalose dihydrate, polyethylene glycol (PEG) 1500 and 4000, maltose monohydrate,
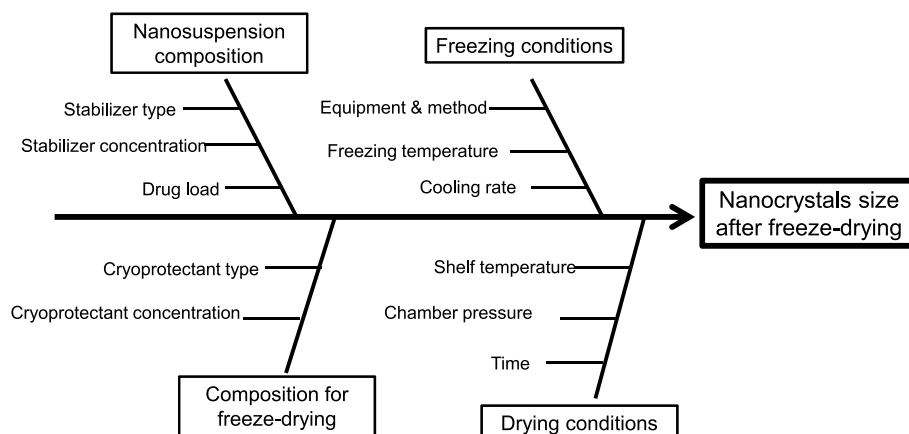

Fig. 1. Fishbone diagram of factors affecting the nanocrystals size of lyophilized nanosuspensions.

maltodextrin D.E. 9-15, inulin, xylitol; Alfa Aesar (Thermo Fisher Scientific, Waltham, MA, USA): D-mannitol.

2.2. Preparation of cilostazol nanosuspension

Detailed description of the preparation of CIL nanosuspension with liquid antisolvent precipitation-sonication method is given in our previous work [34]. Briefly, a 10 mg/mL solution of cilostazol in DMSO (solvent phase) was added by peristaltic pump to water (antisolvent phase) containing equal weight of PVA as stabilizer under magnetic stirring of 600 rpm. The v/v ratio of solvent to antisolvent was 10/90. Following the immediate precipitation, the sample was sonicated for 1–1.5 h under the 100% amplitude of a 130 W probe sonicator (VCX-130, Sonics & Materials Inc., Newtown, CT, USA).

2.3. Determination of Tg' values of cryoprotectant solutions

Glass transition temperature of maximally freeze-concentrated fraction (Tg') for cryoprotectants at 10% w/v was determined in 0.1% PVA aqueous solutions with differential scanning calorimetry (DSC). The measurements were performed on a DSC4000 Perkin-Elmer calorimeter, under a nitrogen atmosphere, using the cycle of cooling the solution from +20 to −70 °C at 2 °C/min, and subsequently a reheating cycle back to +20 °C at 2 °C/min. The instrument was calibrated for temperature and heat flow with two point calibration method using indium and zinc reference samples and scan rate 10 °C/min prior to measurements of studied samples.

2.4. Freeze-drying of cilostazol nanosuspensions

All freezing and lyophilization studies were carried out using an Epsilon 2–4 LSCplus lyophilizer (Martin Christ, Osterode am Harz, Germany) in open 2R or 10R vials with fill depth of 1–2 cm. The condenser temperature was kept in the range from −90 to −80 °C and each process where shelf-ramped freezing was employed started with samples equilibration for 15 min at +20 °C.

2.4.1. Preliminary study

The preliminary study was carried out to explore the feasible primary drying parameters space and observe formulation behavior when using directly the precipitated-sonicated CIL nanosuspension without prior organic phase removal (10% DMSO). For simplification, only a few selected cryoprotectants of different type were used at this stage based on the results of freeze-thaw study (see Supplementary Materials): fructose as monosaccharide, lactose as disaccharide, inulin as polysaccharide, mannitol as polyol, glycine as amino acid and gum arabic as high viscosity polymer). The final concentration of the cryoprotectant was checked in the range 0.1–5% w/v. The operational settings in three preliminary experiments are given in Table 1. The hold time at target freezing shelf temperature was 2 h and primary drying was performed for 30 h.

2.4.2. Main study – the effect of formulation and processing parameters on redispersibility

The main study was performed to assess the influence of freezing and primary drying parameters on the particle size of redispersed CIL nanocrystals and cake appearance. At this stage of experiment, nanosuspensions were used after the removal of DMSO by overnight dialysis (SnakeSkin tubing, MWCO 10K, Thermo Fisher Scientific, Waltham, MA, USA), with approximately 5 times higher volume of PVA solution (antisolvent phase) saturated with cilostazol as dialysis medium. The effect of each processing variable was checked for matrix-free CIL nanosuspension and for twelve cryoprotectants: sucrose (SUC), glucose (GLUC), trehalose (TRE), lactose (LAC), fructose (FRU), inulin (INU), maltodextrin (MDX), mannitol (MANN), xylitol (XYL), glycine (GLI), gum arabic (ARAB) and PEG 1500. With the exception of limits imposed by inulin solubility, for every set of operating conditions the concentration of cryoprotectants was 1 (except one setup), 5 and 10% w/v.

Two shelf temperatures (−70 vs. −40 °C) and two shelf cooling ramp rates (0.5 vs. 2 °C/min) during the freezing stage, as well as two primary drying shelf temperatures (−40 vs. −25 °C) were thoroughly studied in five combinations of settings (noted from 'A' to 'E', Table 1). At this stage of experiments the hold time at the target freezing temperature (2 h), primary drying time at target temperature (24 h) and primary drying chamber pressure (0.05 mbar, corresponding to −48 °C at water sublimation interface) were kept constant. At the transition from freezing to primary drying stage the shelf temperature was raised to target value at the rate of 0.5 °C/min. For the sake of time saving, no secondary drying protocol was applied in the main study, since there is low likelihood of nanoparticle aggregation after the majority of the frozen liquid phase has been sublimated.

After the effects of formulation and processing variables were evaluated, optimal settings in terms of CIL nanocrystals redispersibility and cake appearance were identified and additional lyophilization cycles on selected formulations were performed for further characterization studies, i.e. morphology, solid state properties, residual DMSO and moisture levels and cilostazol dissolution. For the 'characterization' runs, the primary drying time was extended to 52 h to compensate for the higher volumes to be sublimated. Moreover, secondary drying step was added with shelf temperature increase at 0.2 °C/min (5 h duration) to 20 °C and target hold for 7–8 h.

2.4.3. Statistical evaluation of the effect of studied factors

Statistical evaluation of the results with redispersibility index (RDI) as response was performed using Statistica 13.1 (StatSoft Polska, Cracow, Poland). To detect whether the type of cryoprotectant as a qualitative variable has a significant effect on RDI value, one-way ANOVA with cryoprotectant type as categorical grouping variable was performed separately for each studied set of conditions and concentration. F-Welch test was employed where variance inhomogeneity according to Brown-Forsythe test had been detected ($p < 0.05$). Differences between cryoprotectants were considered as significant at $p < 0.05$. In such cases, to elucidate and compare the RDI between these groups in detail, posthoc Tukey tests ($p < 0.05$) were performed. To assess the impact of quantitative variables on RDI, i.e. cryoprotectant concentration,

Table 1

Freezing and primary drying settings for the preliminary study and main study on freeze-drying of cilostazol nanosuspension.

Freeze-drying conditions		Freezing temperature [°C]	Shelf cooling rate [°C/min]	Primary drying temperature [°C]	Chamber pressure [mbar]
Preliminary study	**1**st **run**	−70	2	−40	0.014
	2nd **run**		0.5	−55	0.040
	3rd **run**		2	−40	0.050
Main study conditions	**A**	−70	2	−40	
	B	−40	2	−40	
	C	−40	0.5	−40	
	D	−70	0.5	−40	
	E	−40	2	−25	

freezing temperature, shelf cooling rate and primary drying temperature, separate analyses of Generalized Linear Models (GLM) ANCOVA were carried out for every type of cryoprotectant separately. Statistically significant ($p < 0.05$) main linear effects were detected according to one-way significance tests and parameters estimation (effect coefficients) was used to determine the positive or negative sign of the effect for the abovementioned, significant quantitative factors. According to the software, the GLM analysis involved sigma-limitations and type VI sum of squares.

2.5. Characterization of freeze-dried cilostazol nanocrystals

2.5.1. Particle size distribution and redispersibility index (RDI)

CIL particle size distribution for nanosuspensions and freeze-dried material was measured using laser diffractometry (Mastersizer 3000 equipped with Hydro SV wet dispersion accessory, Malvern Panalytical Ltd., Malvern, UK). Lyophilizates were dispersed in water saturated with cilostazol at the volume corresponding to the liquid sample by gentle manual shaking. The measurement medium was composed of nanosuspension's liquid phase (refractive index 1.35), the particles' refractive and absorption index were set respectively at 1.57 and 0.001 and samples were added to reach obscuration range of ~2–7% [34]. Mean values of six readings were calculated for d10, d50 and d90 parameters.

Since d90 value was considered as the most representative and sensitive to changes due to aggregation or nanoparticle growth, it was the main response of interest in this study. Therefore, redispersibility index (RDI) was calculated as the ratio between the d90 value of redispersed sample and original nanosuspension: *RDI% = (d90 redispersed/d90 original) x 100%*.

2.5.2. Morphology and solid state characterization

The analyses were carried out for selected formulations from 'characterization' freeze-drying runs as described in section 2.4.2. Apart from the lyophilized CIL nanosuspensions, placebo formulations (freeze-dried from solutions of PVA and cryoprotectant without cilostazol nanocrystals) were also evaluated, as well as physical mixtures in the case of solid state assessment.

Scanning electron microscopy (SEM) imaging of selected formulations was performed with Quanta FEG 250 (FEI, Thermo Fisher Scientific, Waltham, MA, USA) microscope under low pressure of 70 Pa and accelerating voltage of 10 kV.

Fourier-transformed infrared (FTIR) spectra were registered in the 4000–400 cm^{-1} range in transmittance scale with the resolution of 1 cm^{-1} for samples compacted with KBr, using a Bruker IFS 66v/S spectrometer (Bruker, Billerica, MA, USA).

X-ray powder diffractometry (XRPD) was carried out on a D8Advance (Bruker, Billerica, MA, USA) equipped with Johansson monochromator (λCu K$_{\alpha1}$ = 1,5406 Å) LynxEye strip detector in 2θ angle range of 4–39, with step value of 0.025 and step time of 1.5 s.

Thermogravimetric analysis (TGA) was performed on TGA8000 Perkin-Elmer instrument, samples were weighted in platinum sample pan and heated in the range from 30 to 1000 °C at 10 °C/min. The instrument was calibrated according to Perkin-Elmer gold standard method using magnetic reference samples and observation of the phase transition from ferromagnetic to paramagnetic state above the intrinsic Curie temperature. DSC was performed in aluminum pans hermetically closed under press. The samples were heated and cooled at 10 °C/min within the temperature range depending on sample decomposition as indicated by TGA, which is different from the conditions used to determine the formulations' Tg' (section 2.3).

2.5.3. Residual solvent and moisture

Residual DMSO levels in nanosuspension, nanosuspension after dialysis and selected freeze-dried nanocrystals formulations from 'characterization' runs were determined with a gas chromatography (GC) method using Agilent 7890B with DM-640 (Agilent, Santa Clara,

CA, USA) column (30 m × 0.53 mm × 3 μm). The carrier gas was helium at the flow rate of 5.58 mL/min, the split was set at 20:1, the temperature was set at 250 °C for dosing chamber and 260 °C for the detector (FID type, 10 Hz), and programmed for the oven (70 °C for 5 min, increase at 15 °C/min to 150 °C, then at 35 °C/min to 260 °C, held for 20 min) Accurately weighed samples of ~100 mg were dissolved in 5 mL of water, filtered through a nylon 0.45 μm filter and injected at the volume of 1 μL. Analysis was run for 33.5 min and DMSO level was determined from calibration curve (0.02–4 mg/mL, R^2 = 0.9999) based on peak area. The LOD and LOQ values were 0.0099 and 0.0301 mg/mL respectively, corresponding to 0.05% and 0.15% for the adopted sampling size.

Residual moisture level in selected formulations and their placebo counterparts without cilostazol nanocrystals was determined with a volumetric Karl Fischer titration method with Aquastar Titrant 5 and Aquastar Solvent for two-component reagent systems (Merck Life Science, Poznan, Poland) on a DL38 titrator (Mettler-Toledo, Warsaw, Poland). Samples of ~200 mg were weighed with accuracy of 1 mg, dissolved or dispersed with sonication in ultrasonic bath in exact volume of methanol for HPLC 99.9%; the water amount determined in the extraction solvent was subtracted as blank in sample measurements. All the volumetric titration method parameters were kept on default levels for the applied titrant and burette type as recommended by the volumetric Karl Fischer titration guidelines.

2.5.4. Cilostazol content and in vitro dissolution testing

Cilostazol % content in selected freeze-dried formulations was determined with a validated spectrophotometric method at 259 nm [34] after dissolving accurately weighed samples in methanol. The analytical evaluation was performed offline in a 10 mm cuvette, with methanol as blank. Method specificity with respect to cilostazol at 259 nm had been confirmed by measuring the absorbance and spectra of placebo components at their target concentrations. The absorption coefficient for cilostazol was 3.9 (as determined by single-point calibration of API standard corresponding to 0.026 mg/mL); the concentration curve had been confirmed as linear up to 0.625 mg/mL with non-significant intercept and r = 0.999.

Evaluation of the dissolution kinetics of cilostazol nanocrystals from selected freeze-dried matrices was performed in a USP 2 apparatus (Erweka DT 126 Light) in non-sink conditions. The final achievable concentration of cilostazol would amount to 6 μg/mL, which is equal to the drug's equilibrium solubility at 37 °C [34]. This type of non-sink conditions has been found to best discriminate the dissolution behavior of nanosuspensions [45]. Lyophilizate samples corresponding to 3 mg of pure cilostazol were carefully sprinkled on the surface of 500 mL of water as dissolution medium at 37 °C, paddle speed was set at 25 rpm. At time points of 1, 3, 5, 10, 15, 20, 30 and 60 min 5-mL samples were withdrawn without replacement and filtered without delay through Anotop Plus 0.02 μm syringe filters (with first 2–3 mL of the filtrate discarded); changes to medium volume and total drug amount were considered in calculations. CIL concentration was determined spectrophotometrically to calculate % dose dissolved against deionized water as blank with the same method as described above.

3. Results and discussion

3.1. Determination of Tg' values of cryoprotectant solutions

Temperature data for thermal events recorded on DSC during the cooling and reheating of various cryoprotectant solutions are presented in Table 2 and Fig. S2. The glass transitions of maximally freeze-concentrated fraction are generally in agreement with literature data, although none were found for gum arabic and PEG. This would also suggest that the presence of additional polymer, i.e. PVA as the nanosuspension stabilizer in the antisolvent phase (at the concentration 1000-fold lower than the cryoprotectant's amount) does not affect the

Table 2
Thermal events registered during DSC cooling and heating scans of cryoprotectant solutions between +20 and −70 °C.

Cryoprotectant	Ice crystallization peak [°C]	Tg' [°C]	Crystallized solute melting peak [°C]	Tg' [°C], literature data
SUC	−18.1	−33.8	–	−31 [11]; −31.9 [46]; −37.9 [47]
GLUC	−16.1	−41.7	–	−43 [11]; −41 [46]
TRE	−16.4	−29.6	–	−29 [11]; −29.8 [46]; −34.2 [47]
LAC	−13.8	−28.4	–	−28.7 [46]
FRU	−15.7	−43.8	–	−41.5 [46]
INU	−14.7	−22.7	–	−32 to −15 [48]; −21.2 (1.8 kDa) to −17.8 (4 kDa) [49]
MDX	−14.2	−11.3	–	−21.97 (D.E. 38) to −12.09 (D.E. 14) [50]
MANN	−15.6	−29.5	−33.1	−29.6 [46]; −26.2 [47]; Tg' −32 and −25, crystallization at −22 [51]
XYL	−16.7	–	–	−46 [46]
GLI	−13.9	–	–	not detected [46]; eutectic melting at −4.37 [47]
ARAB	−14.5	−14.5	–	n/a
PEG 1500	−14.4	–	−14.7; - 48.1	

Tg'. In the case of glycine and xylitol, no thermal events besides ice crystallization and melting were observed in the scanned temperature range. In PEG 1500, two peaks (beside ice crystallization) were observed, which might indicate that the polymer consisted of two independently crystallizing fractions.

For the majority of the investigated cryoprotectants, the Tg' values are above −40 °C, which is common primary drying temperature in typical lyophilization processes [52]. The exceptions are fructose, glucose and possibly xylitol – in these cases relatively high drying temperature might induce matrix devitrification and cake collapse. While nanoparticle immobilization in glass matrix is considered one of the possible mechanisms of preventing their aggregation during freeze-drying [11], it has been proven that drying below Tg' of the cryoprotectant is not always necessary if nanocrystals are sufficiently protected by steric stabilization [12]. With this consideration, in the current investigation formulations containing FRU, GLUC and XYL were consistently lyophilized above their Tg', while for other cryoprotectants comparison was also made of primary drying temperatures above and below this value.

3.2. Freezing and primary drying

Before full freeze-drying cycles, freeze-thaw studies were performed with the range of cryoprotectants to assess whether freezing step itself could force aggregation of cilostazol nanoparticles. The results are described in detail in Supplementary Material. Briefly, the redispersibility of frozen samples appeared satisfactory, as the majority retained similar value of d90 (1.61 μm) to the original suspension, with mean relative difference mostly lower than 10%. RDI values of nanosuspension alone and with 0.2% w/v of cryoprotectants were close to 100%, apart from samples with PEG 4000, which was excluded from further studies. Regardless of freezing temperature and shelf cooling rate in freeze-thaw experiments (see Supplementary Material), mostly low RDI proved that cilostazol nanosuspension was robust and insensitive towards freezing stress itself, even when no cryoprotectant was added. This observation reinforces the idea that proper choice of stabilizer (in this case, PVA) is crucial for the prevention of aggregation and that an optimal stabilizer may be sufficient protection during freezing [16,18, 35] The resistance of the formulations studied by freeze-thawing with relatively low amount of cryoprotectants indicates that any aggregation events occurring during the freeze-drying of cilostazol nanosuspensions would rather result from the sublimation stress during primary drying instead of the freezing step.

3.2.1. Results of preliminary study

The preliminary study was carried out with the main intention to explore the feasibility of freeze-drying of bottom-up generated nanosuspension without the removal of solvent phase (10% DMSO) due to conflicting reports on the use of this solvent in lyophilization processes. On the one hand, while dimethyl sulfoxide has a high boiling point (189 °C) and low vapor pressure at room temperature, being unsuitable for evaporation, it can be effectively sublimated according to an advantage of its high freezing point (18.4 °C) [53]. Pharmaceutical formulations have been successfully freeze-dried either from pure DMSO [54,55] or its mixture with TBA [56]. On the other hand, lyophilization of DMSO mixtures with water may be more challenging depending on the composition, since eutectic point for this organic solvent contents between 50 and 70% is located in the range of approximately −70 to −60 °C [57]. Kunz et al. subjected water-DMSO mixtures to freeze-dry microscopy, which revealed nucleation at −31.1 °C, −66.8 °C and −69.4 °C for DMSO concentrations of 20, 40 and 80%, respectively. When PVP was added to the mixtures, extremely slow sublimation and melting was observed under 100 mTorr pressure for 20% mixture at −40 °C and at −70 °C for 80% DMSO. The authors concluded that due to this behavior only extremely low (1%) and high (99%) concentrations of this solvent may be freeze-dried under reasonable typical conditions in commercial equipment [58]. However, there are reports of lyophilization processes where melting was avoided. In a study on cell preservation, an aqueous formulation containing 5% DMSO (apart from sugar, albumin and PVP) was examined in the primary drying temperature range between −48 and −20 °C at 200 mbar, where it was found that the material did not dry successfully over −30 °C [59]. In a similar way, using the primary drying temperature of −50 °C followed by −30 °C for 24 h each enabled successful drying of a serum albumin formulation containing less than 10% DMSO [60]. There also exist examples where dry material was obtained, but DMSO presence negatively affected product quality. For instance, after primary drying of mixtures containing up to 4% DMSO at −35 °C and 0.01 mbar for 20 h, the solvent was not removed from samples [61]. Finally, in the field of drug nanocrystals, meloxicam nanosuspension precipitated with 20% DMSO could not be successfully redispersed after lyophilization [62], while in a study on breviscapine nanosuspension, this solvent had been removed by centrifugation immediately after sonoprecipitation and its effect in freeze-drying was therefore not investigated [63].

The first of the preliminary cycles was run with freezing to −70 °C at shelf-ramped cooling of 2 °C/min, with primary drying for 30 h at the shelf temperature −40 °C and deep vacuum of 0.014 mbar (corresponding to the range of about −60 to −54 °C at the sublimation front). The majority of samples was not dried and some were dried partially as

evident from the reduced liquid volume. According to resistance sensor, a drop in product resistance corresponding to melting during the primary drying section was registered. Of six cryoprotectants tested at 0.1–5% w/v only two combinations resulted in dry material, although with inelegant cake form: 5% MANN (inhomogeneous, fibre-like spongy structures) and 5% GLI (flat disk lifted from the bottom to the level of the fill volume). In the next preliminary run the shelf temperature during primary drying was further reduced to −55 °C to mitigate the risk of melting. Moreover, to facilitate sublimation vacuum was set to 0.04 mbar and cooling rate during freezing stage was reduced to 0.5 °C to promote growth of larger ice crystals. This procedure did not change the results, with only 5% MANN and 5% GLI producing dry material.

For this reason, it was finally decided to compare the behavior of original nanosuspension with the nanosuspension where the majority of DMSO had been removed by dialysis (content reduced from 12% to 2%). To exacerbate potential differences between different organic levels, cautious drying conditions were disregarded in this case, and the process was carried out according to the set of conditions "A" intended for the main lyophilization study: freezing at 2 °C/min to −70 °C, primary drying at −40 °C and 0.05 mbar (Table 1). In order to further test the systems' performance with hindered sublimation rate, cryoprotectant concentrations were raised to the levels used in the main study (5 and 10%), as higher solids content increases dry layer resistance [52]. The difference between nanosuspensions pre- and post-dialysis was remarkable – almost all dialyzed samples were successfully dried, while for the original nanosuspension only MANN and GLI formulations, similar to previous preliminary tests. Nevertheless, their lyophilizate appearance and homogeneity was markedly improved when dimethyl sulfoxide had been removed (Fig. 2).

The current results corroborate the recommendations made by Kunz et al. regarding the necessity to reduce DMSO contents for effective lyophilization [58]. The organic concentration of ~10% proved too high for liquid removal – probably because as the sublimation of ice progressed, the proportion of DMSO gradually increased, which might have resulted in the composition ranges with deep eutectic point depression and consequently – melting during the primary drying phase [57]. Therefore, the effects of cryoprotectants, freezing conditions and drying temperature were studied for nanosuspensions after dialysis. It is

however interesting to note the divergent behavior of formulations with mannitol and glycine, where liquid was sublimated regardless of the conditions even at high levels of DMSO. This may probably relate to the fact that both these popular cryoprotectants are known as crystallizing excipients. When solutes crystallize upon freeze-concentration, the interstitial spaces between ice crystals are occupied by a mixture of small crystals of ice and solute, and almost all water in the sample is in the frozen state. On the other hand, for amorphous excipients the interstitial region contains the solid solution of concentrated solutes and unfrozen water [64]. It might be tentatively speculated that in the crystalline matrix, the crystals of water and DMSO are spatially separated to some extent and may be able to sublimate independently, without excessive shifting to the phase composition where melting occurs at typical lyophilization temperatures.

3.2.2. Main study – effects of formulation and processing parameters on redispersibility

For a thorough investigation and for the comparison of protection against freezing and drying stresses, a similar array of cryoprotectants was investigated as in the freeze-thaw study (see Supplementary Material). The explored concentrations of 5 and 10% w/v were chosen based on the values typically reported as optimal for the prevention of nanocrystals aggregation within the premise that higher cryoprotectant content is usually required for efficient stabilization [13,37,39,40,43, 65]. For comparison purposes, 1% of matrix former was also checked to verify if the solute content in the formulation could be reduced without compromising the redispersibility.

For the freezing temperature, −40 °C was considered as the recommended, 'default' value [52], being also the same target primary drying shelf temperature, ensuring typical and conservative drying conditions [21]. For comparison, −70 °C was chosen as a more aggressive freezing variant, simultaneously being below the Tg' value of all the studied cryoprotectants (Table 2). Based on the freeze-thaw results (see Supplementary Material), shelf-ramped cooling method was employed to compare the cooling rates typical for commercial freeze-driers, i.e. 0.5 vs. 2 °C/min. The rationale behind the evaluation of this parameter was its governance of supercooling conditions and the size of ice crystals and interstitial spaces where CIL nanoparticle aggregation could take place during sublimation.

Regarding the primary drying shelf temperature, −40 °C was chosen as a conservative, yet reasonably useful setting for the avoidance of excessive processing times, where the majority of studied cryoprotectants is expected to remain vitrified. This was compared against primary drying at −25 °C to verify whether temperatures above excipients' Tg' result in worse nanocrystals redispersibility. Simultaneously, this value would permit relatively faster processing while remaining safely below the freezing point determined by the cryo-DSC analysis (Table 2).

The RDI values and cake descriptions are collected in Table 3 for the formulations with different cryoprotectants studied at different conditions to evaluate the impact of the matrix former type, concentration, freezing temperature, cooling rate and primary drying temperature. Cilostazol PSD was not measured for the samples where persistent aggregation upon reconstitution was visually detected.

Despite using the same formulation compositions and control of the processing parameters, the lyophilization of cilostazol nanosuspensions in some cases seemed to suffer from poor repeatability and unpredictable effectiveness. In spite of the removal of DMSO by dialysis, some of the samples did not dry at all, while in other cases – one unit of the same formulation was effectively dried while another still remained liquid. This might be probably attributed to lack of homogeneity related to different vial locations on the lyophilizer shelf [52]. Evidently, the formulations containing 1% of matrix formers tend to sublimate slowly, as only drying at −25 °C resulted in producing solid material. The reason for this behavior is unclear, considering that if there were difficulties in sublimation to be expected, it would occur at the opposite end of the concentration range, where high solids content in the formulation would

Fig. 2. A comparison of lyophilizate appearance when freeze-drying the original nanosuspension and nanosuspension from which DMSO had been removed by dialysis.

Table 3

Freeze-drying conditions, cake appearance and values of redispersibility index (mean ± SD, n = 2) of nanosuspensions lyophilized with different cryoprotectants in the main study. '*' denotes results where only one out of two samples was successfully dried.

Freeze-drying condition		A	B	C	D	E
Freezing temperature		−70 °C	−40 °C	−40 °C	−70 °C	−40 °C
Cooling rate		2 °C/min	2 °C/min	0.5 °C/min	0.5 °C/min	2 °C/min
Drying temperature		−40 °C	−40 °C	−40 °C	−40 °C	−25 °C
Cryoprotectant	Cake appearance	RDI [%]				
none	thin film in the middle of vial height			aggregated		
SUC 1%	no cake, sediment on vial walls	n/a		not dried		519 ± 287 (722 vs. 317)
5%	collapsed, flat, translucent and glossy (A-D); rough (E) with sediment on vial walls	109 ± 23	102 ± 5	100 ± 5	105 ± 1	113 ± 8
10%	collapsed, flat (A) or with raised edges (B-E), translucent and glossy (B-D) or white and opaque (E)	104 ± 0.4	107 ± 2	101 ± 0	103 ± 2	101 ± 0
GLUC 1%	no cake, sediment on vial walls	n/a		not dried		239 ± 174 (116 vs. 362)
5%	collapsed, flat, translucent and glossy cake (A, B, E) and/or sediment on vial walls	136 ± 1	102 ± 1	99 ± 0.4	105 (=1)	116 ± 0.4
10%	collapsed, flat, translucent and glossy	92 ± 0	101 ± 0	97 ± 6	99 ± 1	103 ± 6
TRE 1%	semisolid sediment on vial walls	n/a		not dried		790 ± 411 (1080 vs. 499)
5%	slightly (A) or entirely collapsed (B-E), partly translucent	87 ± 9	97 ± 4	98 ± 1	108 ± 4	109 (n = 1)
10%	slightly collapsed, white and opaque	82 ± 0	97 ± 1	101 ± 3	101 ± 1	124 ± 0
LAC 1%	semisolid sediment on vial walls	n/a		not dried		393 ± 73
5%	collapsed in the middle with raised edges (A,C); collapsed, flat (B, D, E)	156 ± 40	98 ± 6	139 ± 11	106 ± 2	107 ± 6
10%	collapsed in the middle with raised edges, white and opaque	97 ± 6	98 (n = 1)	201 (n = 1)	119 (n = 1)	216 (n = 1)
FRU 1%	semisolid sediment on vial walls	n/a		not dried		275 ± 94
5%	collapsed, glossy, smooth, semisolid (A, E) or collapsed, flat, rough cake with sediment on vial walls (B, C, D)	94 ± 12	102 ± 6	96 ± 1	108 ± 7	101 ± 1
10%	collapsed, glossy, smooth, semisolid	96 ± 16	103 ± 14	102 ± 2	109 ± 9	103 ± 0
INU[a] 1%	semisolid sediment on vial walls	n/a	109*	not dried		192*
5%	slightly collapsed, white and opaque (A, B, C); collapsed with shrinkage (D) or rough surface (E)	aggregated	101 ± 0	128 ± 16	aggregated	
MDX 1%	semisolid residue on vial walls	n/a		not dried		176*
5%	homogenous, smooth, white and opaque, with slight shrinkage (A, B, E) or collapse and shrinkage (C, D)	96 ± 3	97 ± 9	112 ± 10	298 ± 226 (458 vs. 139)	122 ± 11
10%	homogenous, smooth, white and opaque	not dried	107 ± 11	110 ± 8	155 ± 64 (201 vs. 110)	124 ± 11
MANN 1%	loose lump with sediment on vial walls	n/a		aggregated		528, aggregated
5%	homogenous, smooth (A, D) or slightly porous (B, C, E); white and opaque	159 ± 1	134 ± 11	156 ± 9	aggregated	171 ± 1
10%	homogenous, smooth, white and opaque	152 ± 2	217 ± 53	384 ± 57	339 or aggregated	186 ± 5
XYL 1%	semisolid residue on vial walls	n/a		not dried	not dried	174 ± 53
5%	collapsed, glossy, rough, semisolid (A) or semisolid residue on vial walls (E)	91 ± 3				106 ± 3
10%		90 ± 4			107 ± 9	115 ± 12
GLI 1%	loose lump with sediment on vial walls (B, D) or thick, cracked film in the middle of vial height (D)	n/a	151 ± 7	189 ± 8	169 ± 13	140 ± 14
5%	cracked, slightly shrunken, white and opaque	267 ± 95	109 ± 8	124 ± 15	161 ± 32	116 ± 16
10%	homogenous, smooth, white and opaque	376 ± 57	133 ± 17	aggregated		328 (n = 1)
ARAB 1%	frayed film in the middle of vial height	n/a		not dried		aggregated
5%	homogenous, smooth, creamy white and opaque, slightly shrunk	298 ± 59	267 ± 67	189 ± 31	aggregated and flocculated	
10%		18*	1366 ± 495	1615 ± 280		
PEG 1%	thin film (B-D) of foam-like film (E) in the middle of vial height	n/a	aggregated	829*	aggregated*	194 ± 36
1500 5%	cracked, slightly shrunk, white and opaque (A, D) or foam-like film (E) in the middle of vial height	86 ± 1		not dried	247 ± 134 (152 vs. 342)	181 or aggregated
10%	homogenous, smooth (A, B, C, E) or slightly cracked (D), white and opaque	111 ± 25	98 ± 0	303 ± 292 (97 vs. 510)	111 ± 6	116*

[a] Inulin was used only at the concentrations of 1% and 5% due to limits in solubility.

increase the dry layer resistance, requiring longer primary drying times. Moreover, some formulations appear to be sensitive to drying failures, i. e. samples where xylitol or 5% PEG were used as cryoprotectants. A clear pattern or correlation with processing variables to explain this phenomenon was not observed. Challenges in maintaining lyophilization repeatability and homogeneity are also reflected in differences in the appearance of the solid, at least at matrix concentrations below 10%.

The above deviations somehow restrict the utility of rigorous statistical analyses of the results and prevent any attempts to quantify the relationships between formulation and operating variables with the nanocrystals' particle size. Nevertheless, the potential of redispersibility seems to be affected to a relatively lower degree by repeatability issues than cake appearance. Attempts to determine statistical effects are therefore a kind of approximation to support the analysis of the most prominent relationships. For practical purposes a simplification was adopted where RDI value of 10,000% was arbitrarily attributed to
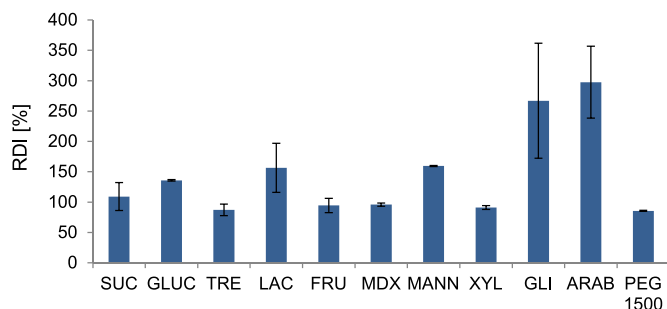
Fig. 3. An example comparison of RDI (%, mean ± SD) between different cryoprotectants at 5% w/v, freeze-dried according to conditions A (freezing temperature −70 °C, cooling rate 2 °C/min, primary drying shelf temperature −40 °C). Results for pure nanosuspension and samples with inulin not measured due to particle aggregation.

samples which formed visible aggregates. Some trends influencing the RDI values could be observed, and the effect of parameters can be cautiously, qualitatively analyzed with the caveat mentioned above.

3.2.2.1. Effect of cryoprotectant type. Undoubtedly, the type of cryoprotectant/matrix former proved to exert strong influence on the RDI value (significant differences at $p < 0.05$ according to ANOVA). While nanosuspension without any additional excipients solidified, the stabilizer alone (PVA) was not able to protect the cilostazol nanoparticles from aggregation during sublimation, regardless of processing conditions. The cryoprotectants in the current study both guided the susceptibility to effective lyophilization (as displayed by the erratic behavior of XYL formulations) and the prevention of CIL particle size increase (Fig. 3). In general, the investigated matrices either ensured redispersion or to the contrary, promoted aggregation. Moreover, those which successfully retained the original cilostazol nanosuspension size tended to do so regardless of the setting of freezing and drying (see the following sections).

The current study confirms the suitability of sugars as matrix formers for the protection from nanocrystal aggregation, demonstrated for a variety of other drug nanoparticles [13,21,66] and commonly attributed to favorable hydrogen bonding interactions according to water replacement hypothesis, or potentially – to interaction with nanosuspension-stabilizing polymer [11,41]. At the same time, the investigation revealed some excipients as entirely unsuitable for the stabilization of freeze-dried cilostazol nanocrystals. One of these is gum arabic, which rendered unacceptably high RDI values despite generally good cake appearance. To the authors' knowledge, the investigation of ARAB for potential cryo-/lyoprotection of drug nanosuspensions has not been described in the publicly available literature. Indeed, the current results do not provide grounds for its use to this purpose, since its high viscosity and low mobility are apparently insufficient to distribute homogenously as a physical barrier to nanoparticle aggregation. Other matrix formers, which would not be recommended based on the current results, are xylitol and inulin. In the case of XYL, while RDI values indicate good preservation of original CIL nanocrystal size, the formulation drying behavior is erratic and the lyophilizate appeared more semisolid/viscous than solid. On the other hand, INU did not prevent aggregation in the majority of runs.

An interesting outcome of the current study on cilostazol nanosuspensions is the poor performance of glycine and mannitol, popular crystallizing excipients. Although the application of GLI or MANN consistently resulted in successful solidification regardless of concentration and conditions (contrary to other tested cryoprotectants), even in the presence of DMSO as discussed in section 3.2.1., increase of cilostazol particle size over 2 μm was always observed. Apparently, MANN and GLI do not provide sufficient protection from sublimation/thermal stress in the case of cilostazol. It might be speculated that this may

potentially be related to the crystallizing nature of both excipients and their inability to immobilize the nanoparticles in glassy matrix, or probably related to an increase in the volume of the crystalline solute shortening the distance between nanocrystals, which in turn could force aggregation. However, this would not be the only mechanism, because PEG is also a crystalline matrix former (Table 2), but such behavior was not observed for this cryoprotectant. It is likely that the excipients' molecular weight and diffusivity may also play a part, affecting phase separation relative to nanoparticles. The current results also reinforce contradictory outcomes on the suitability of mannitol for the freeze-drying of drug nanosuspensions. In several cases, this polyol was identified as the poorest cryoprotectant [14,37], while in other cases it proved to be optimal or at least comparable to sugars [13,39,40,67]. An interesting analysis by Yue et al. revealed that success in stabilizing lyophilized nanosuspensions is correlated to high osmotic pressure of the cryoprotectant, but mannitol deviated from this trend and performed suboptimally even though its osmotic pressure was the highest among the tested substances [21]. The present findings therefore corroborate the complexity of matrix behavior reported in the literature on nanoparticles lyophilization.

3.2.2.2. Effect of cryoprotectant concentration on nanocrystals' redispersibility. An impact of cryoprotectant concentration on the results is evident from the difference between 1% and 5–10% w/v (Fig. 4). For the majority of matrix formers, the application of 1% concentration clearly did not prevent CIL aggregation as demonstrated by distinctly higher RDI compared to higher concentrations. In addition and surprisingly, only at shelf temperature set to −25 °C (conditions 'E', Table 3) during primary drying stage instead of −40 °C, the low concentration samples were able to solidify, as discussed earlier in section 3.2.2.

As a consequence of the dissimilarity of RDI values between 1% and higher cryoprotectant contents, ANOVA detected the effect of matrix concentration as statistically significant ($p < 0.05$) for most excipients. Regarding the comparison of 5% and 10% levels across the range of freeze-drying settings, a generally slight negative trend was observed for the majority of cryoprotectants, although with current datasets statistical significance was not always detected. In other words, 10% of matrix former usually ensured slightly more beneficial, lower RDI values in the case of GLUC, MDX and PEG, while for SUC, TRE, FRU this trend was marginally present for some of the studied lyophilization conditions, while for other settings redispersibility between 5 and 10% was comparable. These results generally confirm the numerous reports that high matrix contents are necessary to prevent the aggregation of nanoparticles during freeze-drying. Depending on the described API nanocrystals and their concentration in the formulation, further increase in cryoprotectant contents is either found to be beneficial for redispersibility [14,21,39,41,42,66] or does not improve the protection when used over a certain threshold amount [37,40,65,68]. In the current
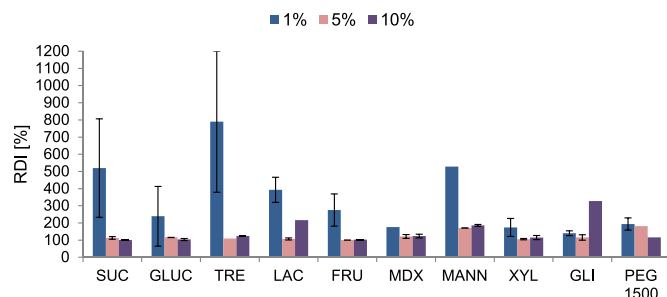

Fig. 4. The effect of cryoprotectant concentration on RDI value (%, mean ± SD where applicable), example freeze-dried according to conditions E (freezing temperature −40 °C, cooling rate 2 °C/min, primary drying shelf temperature −25 °C). Values for gum arabic and inulin not measured due to visible aggregation.

study, while an advantage of 10% cryoprotectant over 5% in terms of maintaining the original nanocrystal size is not always evident, the higher concentration definitely proved better in terms of the lyophilizate appearance and its uniformity over the range of studied processing conditions (Table 3). Interestingly, the opposite has been reported for nanosuspensions stabilized by Poloxamer or Cremophor in sucrose or trehalose matrices [12].

However, some of the investigated matrix formers displayed different influence on RDI. In the case of LAC and MANN, no obvious correlation between concentration and redispersibility was observed, and the effect was not detected as statistically significant. An interesting phenomenon was also observed for GLI and ARAB, where contrary to other cryoprotectants, the statistically significant effect of concentration was positive, i.e. increasing their contents resulted in worse aggregation of cilostazol nanocrystals. To the authors' knowledge, such behavior has not been yet discussed in the publicly available literature on freeze-drying of drug nanosuspensions. The reasons however remain unclear, especially considering the different nature of both excipients (amino acid vs. high MW polymer). It might be speculated that in the case of gum arabic some sort of polymer bridging may have taken place, since in some of the samples flocculation of the excipient itself was observed upon reconstitution. An excess of this high viscosity polymer might possibly have caused permanent agglomeration of the nanoparticles by sticking them together. Regarding glycine, a more complex mechanism would be expected, where factors known to affect cryoprotectant performance such as diffusivity, osmotic pressure and crystallization behavior could play a role yet to be elucidated.

3.2.2.3. Effect of freezing temperature. To the authors' knowledge, this is the only study in the publicly available literature on freeze-drying of drug nanosuspensions where final freezing temperature is considered as a separate variable in complete lyophilization process, apart from the work of Kumar et al., who evaluated −60 °C vs. −40 °C. However, the comparison was made at single experimental points, without systematic investigation against other processing parameters; no influence on indomethacin nanocrystal size was detected [13]. In several other reports on the topic the study of freezing temperature is either reduced to the freeze-thawing stage without considering its impact on the redispersibility after primary drying [14,16,21,41], or it is not treated as an independent parameter, but as a setting joined with freezing time to determine the sample cooling rate [68]. Therefore, the aim of the current work was to fill this knowledge gap by evaluating the influence of freezing temperature in isolation from cooling rate and in relation to the redispersion of the dried material in order to separate aggregation events which could occur during the sublimation stage. Owing to this systematic approach as a complementary investigation to freeze-thaw study (Supplementary Material), the freezing temperature was considered in potential interaction with cryoprotectant type also for the first time to the authors' knowledge.

For the majority of the studied cryoprotectants regardless of the concentration, the freezing temperature (−70 °C vs. −40 °C) did not affect RDI, corroborating the findings of Kumar et al. [13]. Two exceptions were noted: both for INU and MANN freezing temperature displayed statistically significant (p < 0.05), negative effect on redispersibility, i.e. the higher temperature of −40 °C was more effective in preventing CIL nanocrystal aggregation during drying than −70 °C. This is especially notable in the case of inulin, where the influence of this parameter appears to be exerted in an 'all or nothing' manner. At the same drying temperature, the samples frozen at −70 °C (conditions A and D) were clearly aggregated, while those frozen at −40 °C (conditions B and C) displayed satisfying redispersibility index (Table 3). The observed phenomenon might possibly be related to the higher molecular mobility of the excipient at higher temperature, which could allow more effective spatial rearrangement and better coverage and separation of cilostazol nanoparticles. On the other hand, the relationship of this

dependence to the cryoprotectants' properties remains to be elucidated. Both inulin and mannitol did not display divergent thermal behavior in frozen solutions from other matrix formers (section 3.1.), and they do not share common solid state properties - inulin undergoes vitrification, while mannitol is a crystallizing excipient (Table 2). Evidently, the effect of freezing temperature is not related solely to molecular weight either, since it was not observed for PEG 1500 nor even more so for ARAB.

Nevertheless, it is worth noting that freezing temperature should not be neglected as a variable to be studied for the optimization of nanosuspensions lyophilization and warrants further consideration in similar future investigations.

3.2.2.4. Effect of shelf cooling rate. The effect of cooling rate during the freezing stage was generally negligible with the exception of formulations with GLI and MANN, where it was statistically significant (p < 0.05) and negative, i.e. faster cooling rate of 2 °C/min resulted in better, lower RDI than 0.5 °C/min. This is most likely related to the crystallizing character of both excipients, although the same relationship was not observed for crystallizing PEG 1500 – possibly due to differences in molecular weight, diffusivity and phase separation. Faster cooling rate has been proven to accelerate both the nucleation of ice and mannitol [69], and therefore many smaller crystals of water and solute are generated when compared to slower cooling (and lower degree of supercooling). This translates to lower volume of interstitial spaces where nanoparticles could aggregate and therefore – the nanocrystals could be considered as more intimately and homogenously dispersed within crystalline matrix when using faster cooling rates. Still, the success in original CIL size preservation was only relative and both GLI and MANN were suboptimal for the prevention of aggregation.

It is worth noting that the current study is uncommon in its approach to evaluate the influence of shelf ramp rate of a typical commercial lyophilizer during freezing on redispersion after primary drying, let alone in a systematic way for different matrix formers. Other research on cooling rate in the field of nanosuspension lyophilization has so far either restricted to freeze-thaw stage, often even without cryoprotectants [14,16,35,41,68], or employed other types of setup such as freezers or liquid nitrogen [20,43,65], which does not translate easily to practically relevant processes. Nevertheless, the presented results confirm the observations that cooling rate either does not affect redispersibility or that faster freezing is advantageous, although contrary effect has also been observed [41].

3.2.2.5. Effect of primary drying temperature on nanocrystals' redispersibility. A significant (p < 0.05), positive effect of primary drying temperature was recorded only for formulations with one cryoprotectant, inulin, where drying at −25 °C forced aggregation, in contrast to −40 °C (conditions B vs. E, Table 3). The other matrix formers employed in the presented investigation apparently do not differ in their potential to protect CIL nanocrystals from sublimation stress at various drying temperatures, at least in the conservative range tested.

As noted earlier in the literature discussion on the effects of freezing temperature and cooling rate, the influence of drying temperature on nanoparticle redispersibility has not been explored in a systematic way for various cryoprotectants as well. While lower drying temperatures have been generally found to be more beneficial [14,16], as drying below cryoprotectants' Tg' is widely considered necessary for nanocrystal immobilization in vitrified matrix [11], Beirowski et al. proved that with optimal stabilizer choice, this is not necessary [12]. The current study generally supports this conclusion, since no differences in RDI values for the same cryoprotectant type and concentrations were detected between shelf temperatures below and above their Tg' (Table 2). What is more, aggregation was prevented even in the case of fructose and glucose which were consistently dried at temperatures higher than their glass transitions of maximally freeze-concentrated fraction. Still, an external matrix former was necessary at

appropriately high concentration to stabilize CIL nanoparticles size.

3.2.2.6. Summary of the factors study and optimization. The most significant effect on CIL nanoparticles redispersibility was exerted by the type of cryoprotectant and its concentration, while processing variables (freezing temperature, cooling rate, primary drying temperature) influenced the nanocrystal size only for the selected formulations of suboptimal cryoprotectants. The current findings indeed confirm the rule that in freeze-drying of drug nanosuspensions, the formulation plays a decisive role and the impact of operating parameters is secondary [11]. A comparison with the existing literature reports also reinforces the conclusion that many effects seem to be specific for the particular combinations of drug, stabilizer and cryoprotectant [21].

As a result of the systematic study of freeze-drying variables, optimal settings were identified for comparative characterization of the lyophilizates. Based on the lowest RDI values, their repeatability and acceptable cake appearance, three formulations were chosen representing different chemical types of cryoprotectants: 10% TRE (a disaccharide), 10% PEG (a polymer with hydroxyl groups) and 5% MDX (a polysaccharide). The samples were processed according to optimal conditions B, i.e. cooling at 2 °C/min to −40 °C and primary drying at −40 °C. To evaluate the effectiveness of both water and residual DMSO removal, secondary drying step was added with shelf temperature increase at 0.2 °C/min (5 h duration) to 20 °C and target hold for 7–8 h. The CIL particle size distributions of the reconstituted lyophilizates are presented in Fig. 5. In all the cases the majority of the particles retained the size below 1 μm, although the distribution curves were slightly shifted towards higher values. The best results were achieved by trehalose samples due to the best repeatability of the process. In the case of maltodextrin and PEG formulations, a minimal growth of large-micron scale particle fraction could be observed. With these two cryoprotectants, the lyophilization process appeared to be less repeatable, as one out of three samples displayed some degree of aggregation, which translated to increasing the mean d90 value, especially in the case of PEG (4.20 μm vs. 2.08–2.19 μm). Either way, the redispersibility index for TRE and MDX lyophilized nanocrystals is close to 100%, and even below in the case of trehalose, which is probably related to accuracy and repeatability of nanosuspension sampling.

3.3. Characterization of selected formulations of freeze-dried cilostazol nanocrystals

3.3.1. Morphology

The visual appearance of selected optimal samples and their placebo counterparts (lyophilized cryoprotectants in aqueous PVA solutions) are presented in Fig. 6. All the cakes were acceptably elegant, solid, homogenous, without visible differences between formulations containing CIL and free from cilostazol nanoparticles, apart from traces of foaming in the case of PEG.

The SEM images of the three compared formulations and their placebos are presented in Figs. 7–9.

The lyophilized CIL nanosuspensions with all three cryoprotectants clearly differ in matrix morphologies when compared to their placebo counterparts. In the case of TRE and MDX, the freeze-dried nanosuspension consists of continuous, smooth, irregular network of interconnected, spherical-like agglomerates of the carbohydrate. On the other hand, their placebo formulations appear to be made of larger, three-dimensional plates or flakes with porous/spongy internal structure. Interestingly, in the case of placebo MDX quasi regular, crystallite structures could be observed (Fig. 8F), which is surprising given the amorphous character of maltodextrin (see section 3.3.2.). In the case of PEG 1500 nanocrystals formulation, the flakes of the matrix appear thicker, smoother with rounded edges when compared to placebo. The nanosuspension-free lyophilizate of PEG also displays large areas of porous or lamellar internal structures, which seem to be mostly absent from cilostazol-containing samples.

The difference in matrix morphologies between freeze-dried CIL nanosuspensions and placebo formulations suggests that the presence of cilostazol nanocrystals or 2% DMSO (in nanosuspension after dialysis) in certain way modified ice nucleation and growth patterns. To the authors' knowledge, such a comparison has not been presented yet in the publicly available literature on lyophilization of drug nanosuspensions. Thus it is difficult to assess if it is common for drug nanoparticles to exert impact on matrix particles, although it has been demonstrated that different contents of nanocrystals modify the surface and shape of the excipient particles for example in spray freeze-drying [17,70]. On the other hand, it has been established that addition of organic solvents modifies ice crystal habit and sublimation [53]. It is also interesting to note that the observed differences in morphology do not relate to the solid state of the matrix former – in both cases, TRE and MDX were amorphous, while PEG remained crystalline (see section 3.3.2.).
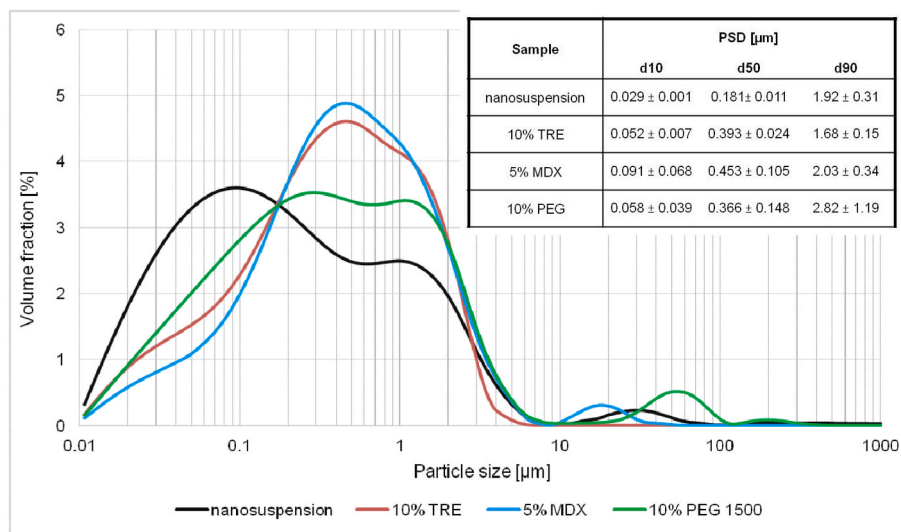
Cilostazol nanoparticles appear to be homogenously and

Sample	PSD [μm]		
	d10	d50	d90
nanosuspension	0.029 ± 0.001	0.181 ± 0.011	1.92 ± 0.31
10% TRE	0.052 ± 0.007	0.393 ± 0.024	1.68 ± 0.15
5% MDX	0.091 ± 0.068	0.453 ± 0.105	2.03 ± 0.34
10% PEG	0.058 ± 0.039	0.366 ± 0.148	2.82 ± 1.19

Fig. 5. Cilostazol particle size distributions of original nanosuspension (after dialysis) and lyophilized formulations selected for optimal characterization cycles.
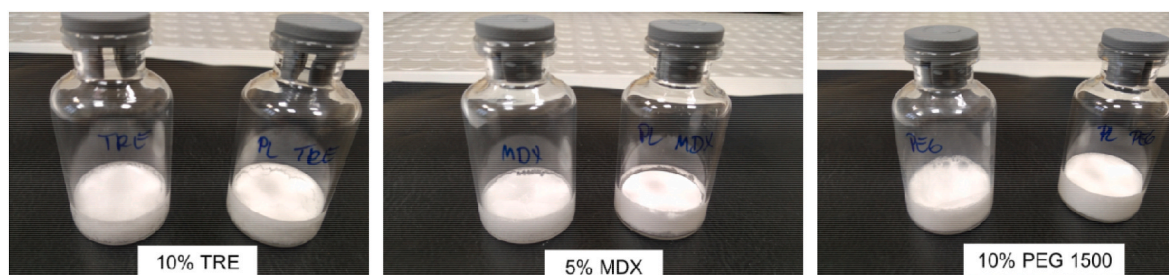
Fig. 6. Cake appearance of cilostazol nanosuspensions lyophilized with selected cryoprotectants (left-side vials) and placebo cryoprotectant formulations (right-side vials).
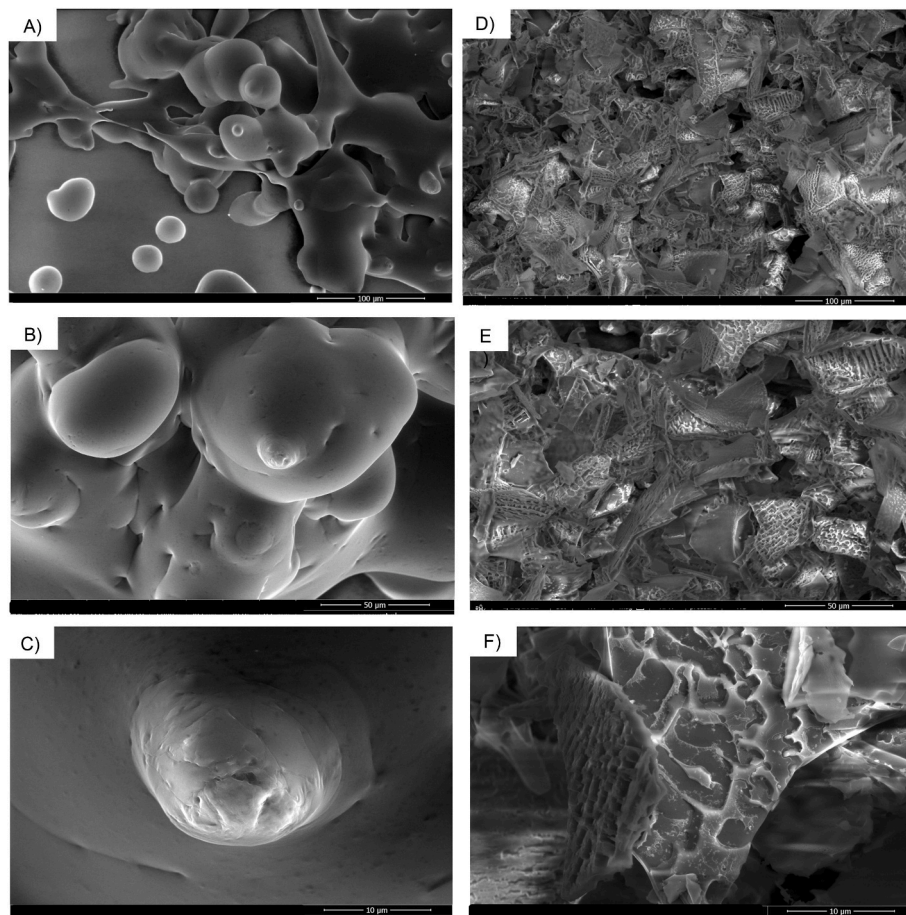

Fig. 7. SEM images: A-C) CIL nanosuspension lyophilized with 10% trehalose; D-F) placebo formulation lyophilized with 10% trehalose. Magnification 1,000×, scale bar 100 μm (A,D), 2000 x, scale bar 50 μm (B,E) and 10,000 x, scale bar 10 μm (C,F).

continuously embedded within trehalose matrix, without signs of aggregation (Fig. 7A–C). On the other hand, in maltodextrin and PEG matrices (Figs. 8 and 9 A-C) CIL nanocrystals can be distinguished in the matrix, either embedded or collected at the surfaces. Contrary to TRE, in several places aggregates appear to have formed, although some degree of separation was retained as evident from satisfactory redispersibility (Fig. 5).

3.3.2. Solid state analysis

Regarding FTIR spectra, no major evident band shifts could be observed in freeze-dried CIL nanosuspension and placebo samples with respect to cryoprotectans as raw materials (Fig. 10 and S3–S5). In the case of trehalose, conversion from crystalline dihydrate into amorphous form occurred, which caused the disappearance of O–H stretching band at 3500 cm^{-1} corresponding to water molecule in the hydrated

pseudopolymorph [71], as well as resulted in more diffuse spectrum. Signals of cilostazol could be observed in freeze-dried nanocrystals at 1669 and 1505 cm^{-1} (C=O stretching and tetrazol N–H bending [72]) quite clearly for PEG matrix, while in MDX they were weaker, and barely visible in the case of TRE matrix. The low intensity of characteristic cilostazol bands can be most likely explained by the low amount of the API in lyophilizates (see section 3.3.3), especially that the situation was similar for simple physical mixtures of CIL, PVA and cryoprotectants (Figs. S3–S5, Supplementary Material).

X-ray diffractograms (Fig. 11) of the samples confirm that maltodextrin and PEG retained their original form during freeze-drying (amorphous and crystalline, respectively), while trehalose solidified as amorphous, as opposed to crystalline dihydrate of raw material. The diffractograms of lyophilized CIL nanosuspensions generally follow the pattern of placebo formulations with minor shifts, and the signal
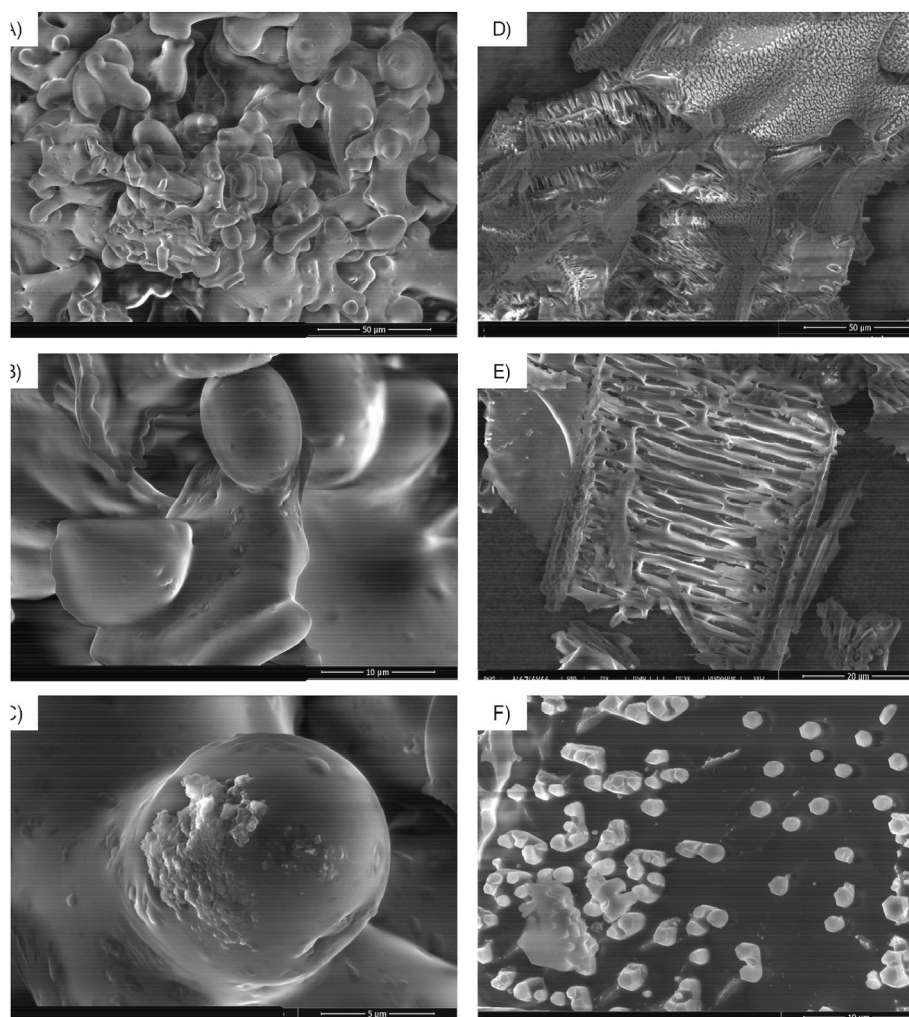
Fig. 8. SEM images: A-C) CIL nanosuspension lyophilized with 5% maltodextrin; D-F) placebo formulation lyophilized with 5% maltodextrin. Magnification 2000 x, scale bar 50 μm (A,D); 5000 x, scale bar 20 μm (E); 10,000 x, scale bar 10 μm (B,F) and 20,000 x, scale bar 5 μm (C).

attributed to matrix formers dominates due to their prevailing amount in the formulation. In the case of two amorphous matrices (Fig. 11B) peaks of distinct intensity above the halo of cryoprotectant were located at 12.47, 15.3, 21.8 and 23.1°. These originate from the crystalline form A of cilostazol [73] and are especially clear in MDX sample, where the drug's content was higher compared to other lyophilizates. There were no characteristic peaks of other polymorphs of cilostazol. In the case of PEG no specific CIL signal was detected, probably due to the intensity of crystalline diffraction pattern of the matrix itself. Therefore, based on the XRPD analysis it can be stated that freeze-drying process did not change the API's polymorphic form in the nanoparticles.

DSC was applied as a complementary technique to study solid state properties as well. However, the samples' behavior during the heating scans does not facilitate straightforward conclusions regarding the polymorphic form of cilostazol due to multiple thermal events and shifts in their location, which is probably related to sensitivity of the results to the samples' thermal history of freeze-drying process. The DSC thermograms are presented in Fig. 12 and detailed discussion is given in Supplementary Material. In the case of freeze-dried CIL nanocrystals with TRE an endothermic peak at 162.43 °C could cautiously be attributed to cilostazol melting of form A, although it would be atypically shifted to higher temperatures when compared to pure crystalline cilostazol and its physical mixture with PVA and trehalose (156 °C). For MDX samples, maltodextrin's own endothermic peaks overlap with the temperature range where cilostazol melting is expected and no typical

endotherms of the API were observed for PEG matrices (see Supplementary Material).

To summarize, in the current study simple DSC proved of limited use to the characterization of polymorphic form of cilostazol due to composite and challenging samples - further studies are planned to elucidate the phase behavior of this drug in mixtures with matrix formers under heating. Nevertheless, it must be stated that in all likelihood the freeze-drying process with different cryoprotectants did not change the original, stable polymorphic form A of cilostazol, although lyophilization of some APIs' bottom-up nanosuspensions has been known to induce partial amorphization [3] and spray drying of CIL nanosuspensions induced some degree of transition to polymorph C under certain conditions [30]. The XRPD clearly points to the crystalline nature of CIL in the lyophilizates, so the dubious events in DSC can be likely attributed to the phenomena related to heating within the matrices during the scan rather than crystallinity changes induced by freeze-drying.

3.3.3. Residual solvent, moisture and in vitro dissolution

The results of residual moisture, residual DMSO and drug content determination are collected in Table 4. CIL content in the lyophilizates is lower than the theoretically expected values of 1% (TRE, PEG) and 2% (MDX), which can be explained by drug loss due to adsorption to equipment during sonoprecipitation and moreover to the membranes during dialysis. It can be clearly seen that the type of matrix former influences the residual levels of both liquid components of the
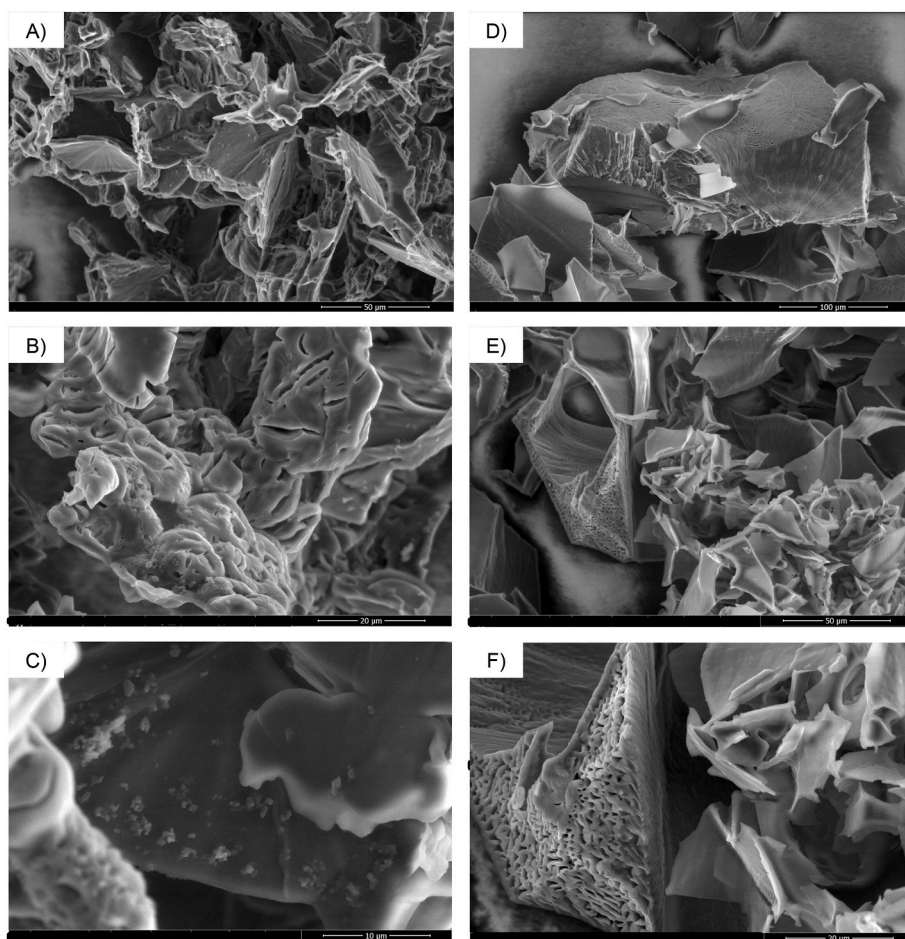
Fig. 9. SEM images: A-C) CIL nanosuspension lyophilized with 10% PEG 1500; D-F) placebo formulation lyophilized with 10% PEG 1500. Magnification 1000 x, scale bar 100 μm (D); 2000 x, scale bar 50 μm (A,E); 5000 x, scale bar 20 μm (B,F) and 10,000 x, scale bar 10 μm (C,E).
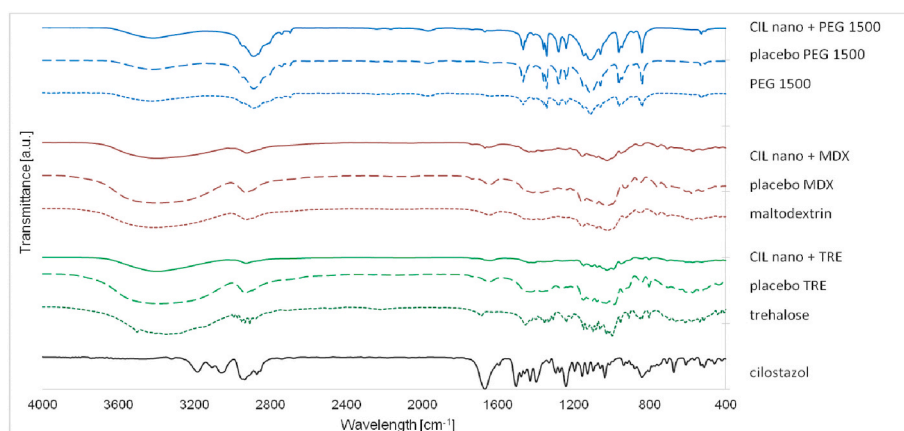

Fig. 10. FTIR spectra of cilostazol, as-received cryoprotectants (dotted lines), freeze-dried placebo formulations (dashed lines) and freeze-dried nanosuspensions with cryoprotectants (solid lines). For individual spectra, see Figs. S3–S5 in Supplementary Material.

nanosuspension, water and DMSO.

The residual moisture level in the lyophilized CIL nanocrystals is generally acceptably low at 1% or less [52]. An interesting correlation was observed: regardless of the cryoprotectant type, the placebo formulations retained roughly twice as much water as the nanocrystals samples. This finding reinforces the differences between matrix structures of the formulations (section 3.3.1). The modification of ice nucleation, growth and sublimation clearly translates not only to the

shape and porosity of the solid, but also to the drying efficiency – the presence of CIL nanocrystals and/or DMSO facilitated water removal. Between different matrix formers, the crystallizing PEG ensured the lowest levels of moisture, especially in contrast to MDX. This is not surprising considering the fact that when using a crystallizing excipient, in principle most of the water is frozen and can be removed almost completely through sublimation. On the other hand, the use of amorphous excipients results in the retention of unfrozen water in solid
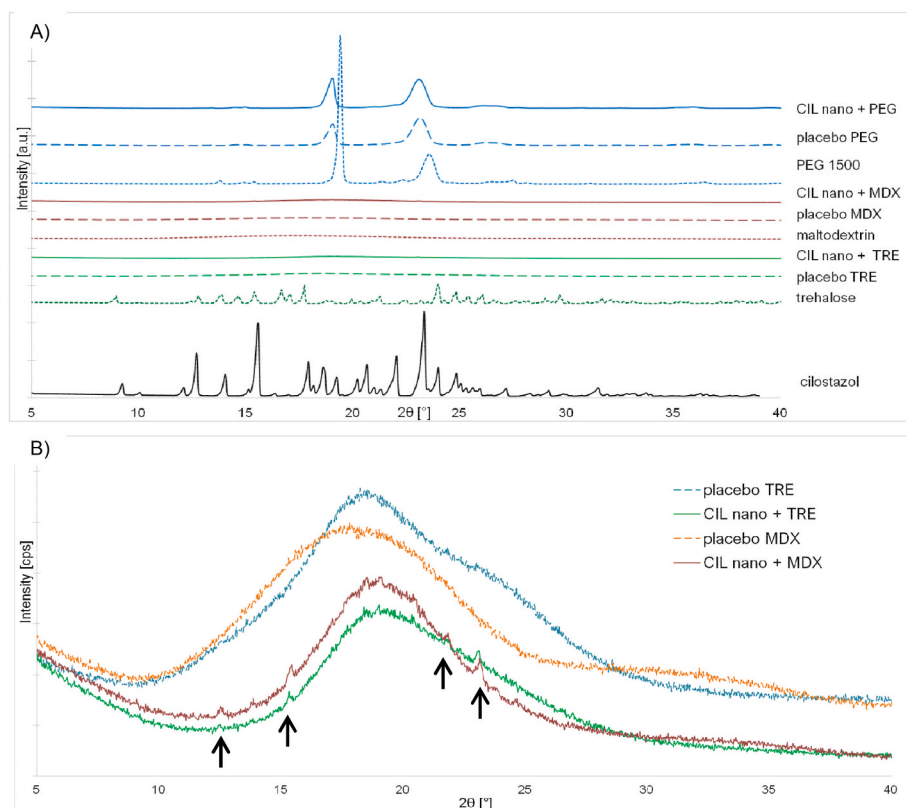
Fig. 11. A) XRPD diffractograms of cilostazol, as-received cryoprotectants (dotted lines), freeze-dried placebo formulations (dashed lines) and freeze-dried nano-suspensions with cryoprotectants (solid lines). B) Close-up of diffractograms of lyophilizates with amorphous TRE and MDX matrices. Arrows indicate characteristic peaks of cilostazol polymorphic form A in nanocrystals.
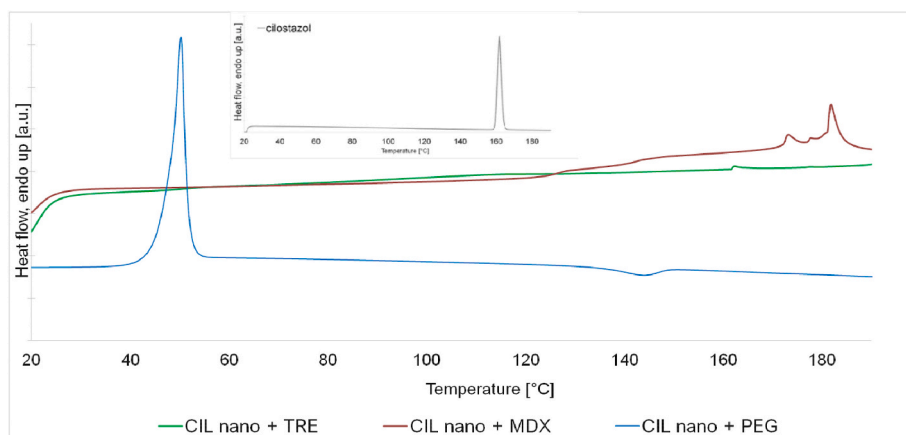

Fig. 12. DSC thermograms freeze-dried cilostazol nanosuspensions with cryoprotectants. Inset: thermogram of raw unprocessed cilostazol.

Table 4
Cilostazol content in lyophilizates, residual moisture and residual DMSO levels for nanocrystals lyophilized with different cryoprotectants and their placebo counterparts.

Sample	Drug content [%]	Moisture content [%]	DMSO content [%]
placebo TRE	n/a	1.148 ± 0.070	n/a
nano + TRE	0.698 ± 0.002	0.575 ± 0.093	9
placebo MDX	n/a	3.672 ± 2.252	n/a
nano + MDX	1.369 ± 0.119	1.075 ± 0.058	13
placebo PEG	n/a	0.631 ± 0.069	n/a
nano + PEG	0.879 ± 0.029	0.363 ± 0.080	0 – below LOD

solution of the vitrified matrix, which needs to be removed by evaporation during secondary drying [64]. Trehalose cake structure proved to be more favorable for this way of water removal when compared to maltodextrin.

A similar mechanism related to differences between cryoprotectant type influenced the residual levels of DMSO as well. The organic content in the original, freshly sonoprecipitated CIL nanosuspension was determined as 12%, after dialysis it was reduced to 2%. The freeze-drying process with crystallizing PEG permitted complete removal of this solvent, as its crystals were readily sublimated. On the other hand, the vitrified matrices of TRE and MDX apparently contained unfrozen DMSO apart from unfrozen water. Although the complete lyophilization cycle reduced the DMSO amount in the solids to about 45% and 31.25%
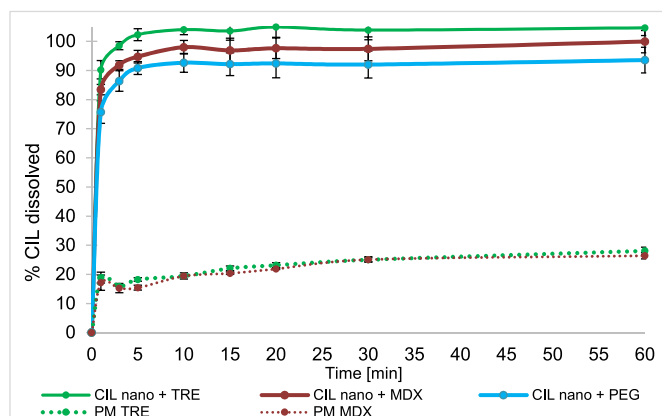
Fig. 13. Dissolution profiles of nanosuspensions lyophilized with cryoprotectants and their corresponding physical mixtures (PM). Results presented as mean ± SD, n = 6 (nano) and n = 3 (PM).

of its starting mass in the dialyzed nanosuspension, respectively, the secondary drying clearly was not able to remove the unfrozen fraction of the organic solvent. This is not surprising, considering its unsuitability for evaporative processes (as discussed in section 3.2.1.). As a result, the residual DMSO levels in TRE and MDX samples remain unacceptably high. It can be concluded that when applying amorphous cryoprotectants, care must be taken to ensure complete removal of the organic solvent during dialysis before lyophilization.

The dissolution profiles of the lyophilizates confirm complete cilostazol nanocrystal dissolution within the first minutes of the test, as opposed to physical mixtures of the cryoprotectant with untreated CIL particles (Fig. 13). The dissolution rate and the plateau levels are correlated with the size of redispersed particles (Fig. 5) in decreasing order TRE > MDX > PEG. The advantage of nanosuspension design for the improvement of dissolution rate was therefore successfully preserved by solidification through optimized freeze-drying.

4. Conclusion

The impact of the formulation and processing variables of freeze-drying on the redispersibility of cilostazol nanocrystals was systematically studied. The nanosuspension stabilized by PVA alone, as well as with cryoprotectants, was insensitive towards cryogenic stress in freeze-thaw study. In the freezing and primary drying investigation it was revealed that the cryoprotectant type and concentration had the strongest significant effect on the nanoparticles redispersibility index. Sugar matrix formers and PEG 1500 proved to be able to successfully prevent aggregation regardless of the processing conditions, while glycine, mannitol, gum arabic and inulin failed to preserve the original nanocrystal size. Of the tested range, a minimum cryoprotectant concentration of 5% w/v was necessary to ensure redispersibility. Processing factors: freezing temperature, cooling rate and primary drying shelf temperature in general did not present significant influence on RDI, although exceptions were noted for some formulations.

As a result of the process characterization, optimal lyophilized nanocrystals of cilostazol were produced and characterized with the use of 10% trehalose or 5% maltodextrin as amorphous matrices, and 10% PEG 1500 as a crystallizing matrix. The stable crystalline form A of cilostazol did not change during the process and the dissolution rate advantage of nanosized particles was successfully preserved. Residual moisture levels were satisfactory, and varied between different matrix formers. On the other hand, in the case of amorphous cryoprotectant formulations, residual DMSO levels were unacceptably high. The study addressed the specific challenges to freeze-drying of nanosuspensions developed with bottom-up methods, i.e. the necessity of organic solvent removal prior to lyophilization and its impact on the processing outcome

in terms of matrix structure, as well as in relation to the different behavior of crystallizing and non-crystallizing excipients.

Author statement

Emilia Jakubowska – conceptualization, methodology, formal analysis, investigation, resources, data curation, writing – original draft, writing – review and editing, visualization, project administration, funding acquisition, Michał Bielejewski – methodology, validation, formal analysis, investigation, resources, data curation, writing – review and editing, visualization, Bartłomiej Milanowski – conceptualization, methodology, validation, resources, writing-review and editing, supervision, Janina Lulek – conceptualization, resources, writing – review and editing, supervision, funding acquisition.

Appendix A. Supplementary data

Supplementary data to this article can be found online at https://doi.org/10.1016/j.jddst.2022.103528.

References

[1] R. Al-Kassas, M. Bansal, J. Shaw, Nanosizing techniques for improving bioavailability of drugs, J. Contr. Release 260 (2017) 202–212, https://doi.org/10.1016/j.jconrel.2017.06.003.

[2] L. Peltonen, J. Hirvonen, Drug nanocrystals – versatile option for formulation of poorly soluble materials, Int. J. Pharm. 537 (2018) 73–83, https://doi.org/10.1016/j.ijpharm.2017.12.005.

[3] A. Bhakay, M. Rahman, R.N. Dave, E. Bilgili, Bioavailability enhancement of poorly water-soluble drugs via nanocomposites: formulation–processing aspects and challenges, Pharmaceutics 10 (2018) 86, https://doi.org/10.3390/pharmaceutics10030086.

[4] W.W.L. Chin, J. Parmentier, M. Widzinski, E.H. Tan, R. Gokhale, A brief literature and patent review of nanosuspensions to a final drug product, J. Pharmacol. Sci. 103 (2014) 2980–2999, https://doi.org/10.1002/jps.24098.

[5] M. Malamatari, S. Somavarapu, K.M.G. Taylor, G. Buckton, Solidification of nanosuspensions for the production of solid oral dosage forms and inhalable dry powders, Expet Opin. Drug Deliv. 13 (2016) 435–450, https://doi.org/10.1517/17425247.2016.1142524.

[6] E. Tashan, A. Karakucuk, N. Celebi, Optimization and in vitro evaluation of ziprasidone nanosuspensions produced by a top-down approach, J. Drug Deliv. Sci. Technol. 52 (2019) 37–45, https://doi.org/10.1016/j.jddst.2019.04.024.

[7] A. Karakucuk, N. Celebi, Investigation of Formulation and Process Parameters of Wet Media Milling to Develop Etodolac Nanosuspensions, Pharm. Res 37 (111) (2020). https://doi-org.libproxy.viko.lt/10.1007/s11095-020-02815-x.

[8] A. Soroushnia, F. Ganji, E. Vasheghani-Farahani, H. Mobedi, Preparation, optimization, and evaluation of midazolam nanosuspension: enhanced bioavailability for buccal administration, Prog Biomater 10 (2021) 19–28, https://doi.org/10.1007/s40204-020-00148-x.

[9] E. Jakubowska, J. Lulek, The application of freeze-drying as a production method of drug nanocrystals and solid dispersions – a review, J. Drug Deliv. Sci. Technol. 62 (2021), 102357, https://doi.org/10.1016/j.jddst.2021.102357.

[10] W. Abdelwahed, G. Degobert, S. Stainmesse, H. Fessi, Freeze-drying of nanoparticles: formulation, process and storage considerations, Adv. Drug Deliv. Rev., 2006 Supplementary Non-Thematic Collection 58 (2006) 1688–1713, https://doi.org/10.1016/j.addr.2006.09.017.

[11] E. Trenkenschuh, W. Friess, Freeze-drying of nanoparticles: how to overcome colloidal instability by formulation and process optimization, Eur. J. Pharm. Biopharm. 165 (2021) 345–360, https://doi.org/10.1016/j.ejpb.2021.05.024.

[12] J. Beirowski, S. Inghelbrecht, A. Arien, H. Gieseler, Freeze drying of nanosuspensions, 2: the role of the critical formulation temperature on stability of drug nanosuspensions and its practical implication on process design, J. Pharmacol. Sci. 100 (2011) 4471–4481, https://doi.org/10.1002/jps.22634.

[13] S. Kumar, R. Gokhale, D.J. Burgess, Sugars as bulking agents to prevent nano-crystal aggregation during spray or freeze-drying, Int. J. Pharm. 471 (2014) 303–311, https://doi.org/10.1016/j.ijpharm.2014.05.060.

[14] Y. Xie, Y. Ma, J. Xu, J. Dan, P. Yue, Z. Wu, M. Yang, Q. Zheng, Roles of cryo/thermal strength for redispersibility of drug nanocrystals: a representative study with andrographolide, Arch Pharm. Res. (Seoul) 39 (2016) 1404–1417, https://doi.org/10.1007/s12272-016-0732-x.

[15] P.-F. Yue, Y. Li, J. Wan, M. Yang, W.-F. Zhu, C.-H. Wang, Study on formability of solid nanosuspensions during nanodispersion and solidification: I. Novel role of stabilizer/drug property, Int. J. Pharm. 454 (2013) 269–277, https://doi.org/10.1016/j.ijpharm.2013.06.050.

[16] P.-F. Yue, J. Wan, Y. Wang, Y. Li, Y.-Q. Ma, M. Yang, P.-Y. Hu, H.-L. Yuan, C.-H. Wang, d-Alpha-tocopherol acid polyethylene glycol 1000 succinate, an effective stabilizer during solidification transformation of baicalin nanosuspensions, Int. J. Pharm. 443 (2013) 279–287, https://doi.org/10.1016/j.ijpharm.2012.12.036.

[17] V. Braig, C. Konnerth, W. Peukert, G. Lee, Can spray freeze-drying improve the re-dispersion of crystalline nanoparticles of pure naproxen? Int. J. Pharm. 564 (2019) 293–298, https://doi.org/10.1016/j.ijpharm.2019.04.061.

[18] R. Mauludin, R.H. Müller, C.M. Keck, Development of an oral rutin nanocrystal formulation, Int. J. Pharm. 370 (2009) 202–209, https://doi.org/10.1016/j.ijpharm.2008.11.029.

[19] A. Touzet, F. Pfefferlé, P. van der Wel, A. Lamprecht, Y. Pellequer, Active freeze drying for production of nanocrystal-based powder: a pilot study, Int. J. Pharm. 536 (2018) 222–230, https://doi.org/10.1016/j.ijpharm.2017.11.050.

[20] B. Van Eerdenbrugh, L. Froyen, J. Van Humbeeck, J.A. Martens, P. Augustijns, G. Van den Mooter, Drying of crystalline drug nanosuspensions—the importance of surface hydrophobicity on dissolution behavior upon redispersion, Eur. J. Pharmaceut. Sci. 35 (2008) 127–135, https://doi.org/10.1016/j.ejps.2008.06.009.

[21] P.-F. Yue, G. Li, J.-X. Dan, Z.-F. Wu, C.-H. Wang, W.-F. Zhu, M. Yang, Study on formability of solid nanosuspensions during solidification: II novel roles of freezing stress and cryoprotectant property, Int. J. Pharm. 475 (2014) 35–48, https://doi.org/10.1016/j.ijpharm.2014.08.041.

[22] H. Fujimura, T. Komasaka, T. Tomari, Y. Kitano, K. Takekawa, Nanosuspension formulations of poorly water-soluble compounds for intravenous administration in exploratory toxicity studies: in vitro and in vivo evaluation, J. Appl. Toxicol. 36 (2016) 1259–1267, https://doi.org/10.1002/jat.3280.

[23] M.-S. Kim, J.-S. Kim, S.-J. Hwang, Enhancement of wettability and dissolution properties of cilostazol using the supercritical antisolvent process: effect of various additives, Chem. Pharm. Bull. 58 (2010) 230–233.

[24] N. Nagai, C. Yoshioka, Y. Ito, Y. Funakami, H. Nishikawa, A. Kawabata, Intravenous administration of cilostazol nanoparticles ameliorates acute ischemic stroke in a cerebral ischemia/reperfusion-induced injury model, Int. J. Mol. Sci. 16 (2015) 29329–29344, https://doi.org/10.3390/ijms161226166.

[25] C. Yoshioka, Y. Ito, N. Nagai, An oral formulation of cilostazol nanoparticles enhances intestinal drug absorption in rats, Exp. Ther. Med. 15 (2018) 454–460, https://doi.org/10.3892/etm.2017.5373.

[26] C. Yoshioka, Y. Ito, N. Nagai, Enhanced percutaneous absorption of cilostazol nanocrystals using aqueous gel patch systems and clarification of the absorption mechanism, Exp. Ther. Med. 15 (2018) 3501–3508, https://doi.org/10.3892/etm.2018.5820.

[27] J.-S. Choi, Design of cilostazol nanocrystals for improved solubility, J Pharm Innov 15 (2020) 416–423, https://doi.org/10.1007/s12247-019-09391-7.

[28] J. Jinno, N. Kamada, M. Miyake, K. Yamada, T. Mukai, M. Odomi, H. Toguchi, G. G. Liversidge, K. Higaki, T. Kimura, In vitro-in vivo correlation for wet-milled tablet of poorly water-soluble cilostazol, J. Contr. Release 130 (2008) 29–37, https://doi.org/10.1016/j.jconrel.2008.05.013.

[29] J. Jinno, N. Kamada, M. Miyake, K. Yamada, T. Mukai, M. Odomi, H. Toguchi, G. G. Liversidge, K. Higaki, T. Kimura, Effect of particle size reduction on dissolution and oral absorption of a poorly water-soluble drug, cilostazol, in beagle dogs, J. Contr. Release 111 (2006) 56–64, https://doi.org/10.1016/j.jconrel.2005.11.013.

[30] X. Miao, C. Sun, T. Jiang, L. Zheng, T. Wang, S. Wang, Investigation of nanosized crystalline form to improve the oral bioavailability of poorly water soluble cilostazol, J. Pharm. Pharmaceut. Sci. 14 (2011) 196–214.

[31] S. Kim, J. Lee, Effective polymeric dispersants for vacuum, convection and freeze drying of drug nanosuspensions, Int. J. Pharm. 397 (2010) 218–224, https://doi.org/10.1016/j.ijpharm.2010.07.010.

[32] I. Aghrbi, V. Fülöp, G. Jakab, N. Kállai-Szabó, E. Balogh, I. Antal, Nanosuspension with improved saturated solubility and dissolution rate of cilostazol and effect of solidification on stability, J. Drug Deliv. Sci. Technol. 61 (2021), 102165, https://doi.org/10.1016/j.jddst.2020.102165.

[33] T. Komasaka, H. Fujimura, T. Tagawa, A. Sugiyama, Y. Kitano, Practical method for preparing nanosuspension formulations for toxicology studies in the discovery stage: formulation optimization and in vitro/in vivo evaluation of nanosized poorly water-soluble compounds, Chem. Pharm. Bull. 62 (2014) 1073–1082.

[34] E. Jakubowska, B. Milanowski, J. Lulek, A systematic approach to the development of cilostazol nanosuspension by liquid antisolvent precipitation (LASP) and its combination with ultrasound, Int. J. Mol. Sci. 22 (2021), 12406, https://doi.org/10.3390/ijms222212406.

[35] J. Beirowski, S. Inghelbrecht, A. Arien, H. Gieseler, Freeze-drying of nanosuspensions, 1: freezing rate versus formulation design as critical factors to preserve the original particle size distribution, J. Pharmacol. Sci. 100 (2011) 1958–1968, https://doi.org/10.1002/jps.22425.

[36] S. Dhat, S. Pund, C. Kokare, P. Sharma, B. Shrivastava, Mechanistic investigation of biopharmaceutic and pharmacokinetic characteristics of surface engineering of satranidazole nanocrystals, Eur. J. Pharm. Biopharm. 100 (2016) 109–118, https://doi.org/10.1016/j.ejpb.2015.12.007.

[37] D. Gol, S. Thakkar, M. Misra, Nanocrystal-based drug delivery system of risperidone: lyophilization and characterization, Drug Dev. Ind. Pharm. 44 (2018) 1458–1466, https://doi.org/10.1080/03639045.2018.1460377.

[38] S. Iurian, C. Bogdan, I. Tomuță, P. Szabó-Révész, A. Chvatal, S.E. Leucuța, M. Moldovan, R. Ambrus, Development of oral lyophilisates containing meloxicam nanocrystals using QbD approach, Eur. J. Pharmaceut. Sci. 104 (2017) 356–365, https://doi.org/10.1016/j.ejps.2017.04.011.

[39] S. Thakkar, D. Sharma, M. Misra, Comparative evaluation of electrospraying and lyophilization techniques on solid state properties of Erlotinib nanocrystals: assessment of In-vitro cytotoxicity, Eur. J. Pharmaceut. Sci. 111 (2018) 257–269, https://doi.org/10.1016/j.ejps.2017.10.008.

[40] L. Wang, Y. Ma, Y. Gu, Y. Liu, J. Zhao, B. Yan, Y. Wang, Cryoprotectant choice and analyses of freeze-drying drug suspension of nanoparticles with functional stabilisers, J. Microencapsul. 35 (2018) 241–248, https://doi.org/10.1080/02652048.2018.1462416.

[41] Y.-Q. Ma, Z.-Z. Zhang, G. Li, J. Zhang, H.-Y. Xiao, X.-F. Li, Solidification drug nanosuspensions into nanocrystals by freeze-drying: a case study with ursodeoxycholic acid, Pharmaceut. Dev. Technol. 21 (2016) 180–188, https://doi.org/10.3109/10837450.2014.982822.

[42] P. Yue, C. Wang, J. Dan, W. Liu, Z. Wu, M. Yang, The importance of solidification stress on the redispersibility of solid nanocrystals loaded with harmine, Int. J. Pharm. 480 (2015) 107–115, https://doi.org/10.1016/j.ijpharm.2015.01.037.

[43] N.-O. Chung, M.K. Lee, J. Lee, Mechanism of freeze-drying drug nanosuspensions, Int. J. Pharm. 437 (2012) 42–50, https://doi.org/10.1016/j.ijpharm.2012.07.068.

[44] J. Lee, Y. Cheng, Critical freezing rate in freeze drying nanocrystal dispersions, J. Contr. Release 111 (2006) 185–192, https://doi.org/10.1016/j.jconrel.2005.12.003.

[45] P. Liu, O. de Wulf, J. Laru, T. Heikkilä, B. van Veen, J. Kiesvaara, J. Hirvonen, L. Peltonen, T. Laaksonen, Dissolution studies of poorly soluble drug nanosuspensions in non-sink conditions, AAPS PharmSciTech 14 (2013) 748–756, https://doi.org/10.1208/s12249-013-9960-2.

[46] H. Meng-Lund, T.P. Holm, A. Poso, L. Jorgensen, J. Rantanen, H. Grohganz, Exploring the chemical space for freeze-drying excipients, Int. J. Pharm. 566 (2019) 254–263, https://doi.org/10.1016/j.ijpharm.2019.05.065.

[47] A. Santoveña, M.J. Piñero, M. Llabrés, Comparison between DSC and TMDSC in the investigation into frozen aqueous cryoprotectants solutions, Drug Dev. Ind. Pharm. 36 (2010) 1413–1421, https://doi.org/10.3109/03639045.2010.487264.

[48] K. Kawai, K. Fukami, P. Thanatuksorn, C. Viriyarattanasak, K. Kajiwara, Effects of moisture content, molecular weight, and crystallinity on the glass transition temperature of inulin, Carbohydr. Polym. 83 (2011) 934–939, https://doi.org/10.1016/j.carbpol.2010.09.001.

[49] W.L.J. Hinrichs, N.N. Sanders, S.C. De Smedt, J. Demeester, H.W. Frijlink, Inulin is a promising cryo- and lyoprotectant for PEGylated lipoplexes, J. Contr. Release 103 (2005) 465–479, https://doi.org/10.1016/j.jconrel.2004.12.011.

[50] S. Corveleyn, J.-P. Remon, Maltodextrins as lyoprotectants in the lyophilization of a model protein, LDH, Pharm. Res. (N. Y.) 13 (1996) 146–150, https://doi.org/10.1023/A:1016006106821.

[51] A. Pyne, R. Surana, R. Suryanarayanan, Crystallization of mannitol below Tg' during freeze-drying in binary and ternary aqueous systems, Pharm. Res. (N. Y.) 19 (2002) 901–908, https://doi.org/10.1023/a:1016129521485.

[52] X. Tang, (Charlie), M.J. Pikal, Design of freeze-drying processes for pharmaceuticals: practical advice, Pharm. Res. (N. Y.) 21 (2004) 191–200, https://doi.org/10.1023/B:PHAM.0000016234.73023.75.

[53] D.L. Teagarden, D.S. Baker, Practical aspects of lyophilization using non-aqueous co-solvent systems, Eur. J. Pharmaceut. Sci. 15 (2002) 115–133.

[54] M.W.J. den Brok, B. Nuijen, C. Lutz, H.-G. Opitz, J.H. Beijnen, Pharmaceutical development of a lyophilised dosage form for the investigational anticancer agent Imexon using dimethyl sulfoxide as solubilising and stabilising agent, J. Pharmacol. Sci. 94 (2005) 1101–1114, https://doi.org/10.1002/jps.20331.

[55] E. Valkama, O. Haluska, V.-P. Lehto, O. Korhonen, K. Pajula, Production and stability of amorphous solid dispersions produced by a Freeze-drying method from DMSO, Int. J. Pharm. 606 (2021), 120902, https://doi.org/10.1016/j.ijpharm.2021.120902.

[56] J. Salazar, A. Ghanem, R.H. Müller, J.P. Möschwitzer, Nanocrystals: comparison of the size reduction effectiveness of a novel combinative method with conventional top-down approaches, Eur. J. Pharm. Biopharm. 81 (2012) 82–90, https://doi.org/10.1016/j.ejpb.2011.12.015.

[57] D.H. Rasmussen, A.P. Mackenzie, Phase diagram for the system water–dimethylsulphoxide, Nature 220 (1968) 1315–1317, https://doi.org/10.1038/2201315a0.

[58] C. Kunz, S. Schuldt-Lieb, H. Gieseler, Freeze-drying from organic cosolvent systems, Part 1: thermal analysis of cosolvent-based placebo formulations in the frozen state, J. Pharmacol. Sci. 107 (2018) 887–896, https://doi.org/10.1016/j.xphs.2017.11.003.

[59] Y. Han, G.B. Quan, X.Z. Liu, E.P. Ma, A. Liu, P. Jin, W. Cao, Improved preservation of human red blood cells by lyophilization, Cryobiology 51 (2005) 152–164, https://doi.org/10.1016/j.cryobiol.2005.06.002.

[60] D. Greiff, B.T. Doumas, T.I. Malinin, B.W. Perry, Freeze-drying of solutions of serum albumin containing dimethylsulfoxide, Cryobiology 13 (1976) 201–205, https://doi.org/10.1016/0011-2240(76)90133-4.

[61] U. Rockinger, C. Müller, F. Bracher, M. Funk, G. Winter, DMSO as new, counterintuitive excipient for freeze-drying human keratinocytes, Eur. J. Pharmaceut. Sci. 160 (2021), 105746, https://doi.org/10.1016/j.ejps.2021.105746.

[62] T. Liu, X. Yu, H. Yin, Study of top-down and bottom-up approaches by using design of experiment (DoE) to produce meloxicam nanocrystal capsules, AAPS PharmSciTech 21 (2020) 79, https://doi.org/10.1208/s12249-020-1621-7.

[63] T. Zhang, X. Li, J. Xu, J. Shao, M. Ding, S. Shi, Preparation, characterization, and evaluation of breviscapine nanosuspension and its freeze-dried powder, Pharmaceutics 14 (2022) 923, https://doi.org/10.3390/pharmaceutics14050923.

[64] J.C. Kasper, W. Friess, The freezing step in lyophilization: physico-chemical fundamentals, freezing methods and consequences on process performance and quality attributes of biopharmaceuticals, Eur. J. Pharm. Biopharm. 78 (2011) 248–263, https://doi.org/10.1016/j.ejpb.2011.03.010.

[65] M.K. Lee, M.Y. Kim, S. Kim, J. Lee, Cryoprotectants for freeze drying of drug nano-suspensions: effect of freezing rate, J. Pharmacol. Sci. 98 (2009) 4808–4817, https://doi.org/10.1002/jps.21786.

[66] R. Shegokar, K.K. Singh, Nevirapine nanosuspensions: stability, plasma compatibility and sterilization, J Pharm Invest 42 (2012) 257–269, https://doi.org/10.1007/s40005-012-0039-y.

[67] H. Zhang, W. Chen, Z. Zhao, Q. Dong, L. Yin, J. Zhou, Y. Ding, Lyophilized nanosuspensions for oral bioavailability improvement of insoluble drugs: preparation, characterization, and pharmacokinetic studies, J Pharm Innov 12 (2017) 271–280, https://doi.org/10.1007/s12247-017-9287-8.

[68] L. Niu, J. Panyam, Freeze concentration-induced PLGA and polystyrene nanoparticle aggregation: imaging and rational design of lyoprotection, J. Contr. Release 248 (2017) 125–132, https://doi.org/10.1016/j.jconrel.2017.01.019.

[69] T.R.M. De Beer, M. Wiggenhorn, A. Hawe, J.C. Kasper, A. Almeida, T. Quinten, W. Friess, G. Winter, C. Vervaet, J.P. Remon, Optimization of a pharmaceutical freeze-dried product and its process using an experimental design approach and innovative process analyzers, Talanta 83 (2011) 1623–1633, https://doi.org/10.1016/j.talanta.2010.11.051.

[70] T. Niwa, K. Danjo, Design of self-dispersible dry nanosuspension through wet milling and spray freeze-drying for poorly water-soluble drugs, Eur. J. Pharmaceut. Sci. 50 (2013) 272–281, https://doi.org/10.1016/j.ejps.2013.07.011.

[71] K. Akao, Y. Okubo, N. Asakawa, Y. Inoue, M. Sakurai, Infrared spectroscopic study on the properties of the anhydrous form II of trehalose. Implications for the functional mechanism of trehalose as a biostabilizer, Carbohydr. Res. 334 (2001) 233–241, https://doi.org/10.1016/s0008-6215(01)00182-3.

[72] M. Pandeeswaran, E.H. El-Mossalamy, K.P. Elango, Spectroscopic studies on the interaction of cilostazole with iodine and 2,3-dichloro-5,6-dicyanobenzoquinone, Spectrochim. Acta 78 (2011) 375–382, https://doi.org/10.1016/j.saa.2010.10.023.

[73] G.W. Stowell, R.J. Behme, S.M. Denton, I. Pfeiffer, F.D. Sancilio, L.B. Whittall, R.R. Whittle, Thermally-prepared polymorphic forms of cilostazol, J. Pharmacol. Sci. 91 (2002) 2481–2488, https://doi.org/10.1002/jps.10240.